Agricultural and Forest Meteorology 354 (2024) 110077

Contents lists available at ScienceDirect

Agricultural and Forest Meteorology

journal homepage: www.elsevier.com/locate/agrformet

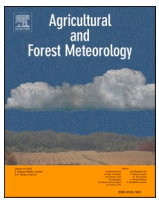

Comparison of two micrometeorological and three enclosure methods for measuring ammonia emission after slurry application in two field experiments☆

Jesper N. Kamp [a,*], Sasha D. Hafner [a], Jan Huijsmans [b], Koen van Boheemen [b], Hannah Götze [c], Andreas Pacholski [c], Johanna Pedersen [a]

[a] Department of Biological and Chemical Engineering, Aarhus University, Aarhus, Denmark
[b] Wageningen University and Research, Wageningen, the Netherlands
[c] Thünen Institute for Climate-Smart Agriculture, Braunschweig, Germany

ARTICLE INFO

Keywords:
Backward lagrangian stochastic model
Integrated horizontal flux
Wind tunnel
Dräger tube method
Dynamic flux chamber
Nitrogen volatilization

ABSTRACT

Ammonia emission following field application of animal slurry is a significant problem for the environment and human health. Accurate emission measurements are crucial for inventories, research, and mitigation. However, there may be large differences between results obtained with different methods. In this study measurement methods were compared in two field experiments: in Denmark (I-AU, trailing hose application, summer, arable land) and the Netherlands (II-WUR, slurry shallow injection, autumn, grassland) over 7 days each. Two micrometeorological methods (Integrated Horizontal Flux (IHF) and backward Lagrangian stochastic (bLS)) and three enclosure methods (Dräger tube method (DTM), wind tunnels (WT), and dynamic flux chambers (FC)) were included in one or both. Measuring in parallel eliminated effects of local factors influencing emission. Relative systematic error in micrometeorological methods (bLS variants and IHF) was estimated from measurements as about 25 % as a standard deviation among methods based on random-effects models. DTM emission measurements were lower than other methods by as much as 34 % of applied TAN compared to bLS. The emission rate measured by IHF followed the same pattern as the other methods soon after slurry application, but total emission was lower (5 % of applied TAN lower than bLS). Different concentration measurement methods used with bLS showed differences of 1–13 % of applied TAN. FC emission was 9–15 % of applied TAN higher than IHF and bLS, but 13 % lower than WT. WT emissions were high and depended on the air exchange rate. Overall relative uncertainty in total emission measured with micrometeorological methods was estimated at 24 and 31 % of the measured value (standard deviation), implying a 95 % confidence interval of about 60 %-160 % of emission measured in a single plot using a micrometeorological method.

1. Introduction

Ammonia (NH_3) is a globally important air pollutant mainly emitted from agricultural sources. High emissions have negative effects on human health by contributing to the formation of fine particulate matter that is a major health concern (Wyer et al., 2022) and the environment by eutrophication, soil acidification, and loss of biodiversity (Sheppard et al., 2011). Furthermore, oxidation of ammonia in the soil can produce nitric oxide and nitrous oxide, with associated effects on air quality and climate change (Zhu et al., 2013).

Synthetic and organic fertilizers are key to meeting increasing global food demand, but increased or intensified use of fertilizers can lead to increasing nitrogen losses to the environment. The agriculture sector accounts for more than 80 % of global ammonia emissions (Wyer et al., 2022). In countries with intensive agricultural production this contribution can be higher, e.g., 96 % in Denmark in 2020 (Nielsen et al., 2022) and 88 % in the Netherlands in 2021 (CBS, PBL, RIVM, 2023). In Denmark, an estimated 26 % of agricultural ammonia emissions originated from manure applied to soil in 2020 (Nielsen et al., 2022) whereas the estimate for the Netherlands was 31 % in 2021 (Bruggen et al.,

☆ (S. D. Hafner), (J. Huijsmans), (K. van Boheemen), (H. Götze), (A. Pacholski), (J. Pedersen).

* Corresponding author at: Aarhus University, Blichers Alle 20, 8830 Tjele, Denmark.
E-mail address: jk@bce.au.dk (J.N. Kamp).

https://doi.org/10.1016/j.agrformet.2024.110077
Received 22 September 2023; Received in revised form 14 May 2024; Accepted 17 May 2024
Available online 29 May 2024

2023). In recent decades, there has been a focus on ammonia abatement involving reduction targets for ammonia within the EU and UN, e.g., The Gothenburg Protocol (UNECE, 1999). Effective and equitable national and international policies, emission inventories, assessment of mitigation options, model development, and research in general all require accurate estimates of emission.

Ammonia emission measurements require measurement of gaseous ammonia concentrations and a method to determine emission using the concentrations. Accurate determination of ammonia concentration is therefore important, but may be challenging, as has been observed in comprehensive comparisons of different instruments. Bobrutzki et al. (2010) compared 11 instruments, where the overall bias ranging from −13 % to 11 %, but with more variability when reaching concentrations below 10 ppb. Twigg et al. (2022) investigated 13 instruments under field conditions and found average biases up to 23 % depending on inlet system and relative standard deviation among instruments of 10 % to 50 %, with highest values at low concentrations. This highlights the difficulty of measuring ammonia concentrations accurately. Any bias in a concentration measurement system will eventually carry over to the emission estimate. Small concentration differences are often used to determine emission rates, and therefore emission error may be proportionally larger than concentration error.

Offline techniques for measuring concentrations, such as acid impingers (where a known quantity of air is pulled through an acid solution to capture all ammonia) or passive samplers (where measured sorbed mass is proportional to the concentration in air that drives the absorption or diffusion rate), are widely used. The offline techniques commonly have limited time resolution and therefore provide limited data on flux dynamics. However, many impingers and passive samplers can be used at the same time to e.g., measure in small plots for comparison of treatments with replicate measurements. Impingers have been used extensively for integrated horizontal flux (IHF) measurements (Goedhart et al., 2020; Huijsmans et al., 2003, 2001). Other techniques used for gaseous ammonia concentrations include ALPHA passive diffusion samplers and passive flux Leuning samplers, which have been used for IHF and ZINST, along with commercial Dräger tubes used for the DTM (Vilms Pedersen et al., 2018). The use of methods for continuously measuring ammonia concentrations with a high time resolution are also used, including cavity ring-down spectroscopy (CRDS) (Kamp et al., 2021), miniDOAS (Sintermann et al., 2016), proton transfer reaction-mass spectrometer (PTR-MS) (Sintermann et al., 2011b), and tunable infrared laser differential absorption spectrometry (QC-TILDAS) (Ferrara et al., 2016).

Emission measurement methods can be divided into enclosure and micrometeorological methods. Enclosure methods use static or dynamic chambers and usually measure over small ($\leq$1 m^2) plots. Examples of enclosure methods include flux chambers (FC) (Bourdin et al., 2014), calibrated passive samplers (Ni et al., 2012), and wind tunnels (WT) (Evans et al., 2018; Pedersen et al., 2020). Dynamic chambers, which also include wind tunnels and flux chambers, are a powerful tool for comparing application methods or slurry treatments because replication is possible. Enclosure methods are generally not suitable for measuring absolute emissions as they modify the environment of the emitting surface compared to ambient conditions by changing air flow (e.g., turbulence, wind speed, and vertical wind profile), along with precipitation, radiation, temperature, and soil conditions (Fowler et al., 2001; Hafner et al., 2024). Enclosure methods normally cover small surface areas, and therefore relatively high random error among plots should be expected, because of variation in soil properties or slurry application rate or coverage. Parallel measurements with identical enclosures have shown that variability can indeed be high relative to the mean flux measured in some intervals but is generally sufficiently low to quantify differences in total emission or even interval flux among slurry types or application methods (e.g., Andersson et al., 2023; Chantigny et al., 2004; Ryden and Lockyer, 1985).

Many different micrometeorological methods have been used after slurry application: the aerodynamic gradient method (AGM) (Kamp et al., 2020), the backwards Lagrangian Stochastic (bLS) method (Häni et al., 2016; Kamp et al., 2021), the dispersion model FIDES (Carozzi et al., 2013; Loubet et al., 2010), eddy covariance (EC) (Ferrara et al., 2016; Sintermann et al., 2011b), IHF method (Goedhart et al., 2020; Huijsmans et al., 2003, 2001), and the ZINST method (Misselbrook and Hansen, 2001; Vilms Pedersen et al., 2018). Micrometeorological measurements average spatial variability over a much larger area than enclosure methods. Unlike enclosure methods, they do not change the surface or atmospheric conditions and are therefore considered suitable for assessing real emission. However, horizontal homogeneity and stationarity are assumed (Fowler et al., 2001), which may cause biases when applying these methods to small sources. Micrometeorological methods offer limited possibilities in the field for comparisons and conducting measurements with multiple plots or replicates with the same conditions.

There is evidence of substantial error in emission measurements. Analysis of a large publicly available collection of measurements of ammonia loss from field-applied slurry showed evidence of consistent differences in measured emission among research institutions or research groups, even after attempting to account for effects of application method, slurry properties, and weather (Hafner et al., 2018). These differences may be caused by a combination of factors, including differences in soil, crop, slurry, and application techniques, but systematic error (bias) in measurement methods likely also contributed. Some studies have compared ammonia emission measurement methods by measuring in parallel in the same field after slurry application, which isolates differences related specifically to measurement methods (Milford et al., 2009; Scotto di Perta et al., 2019; Sintermann et al., 2011a; Vilms Pedersen et al., 2018). The relative difference in cumulative ammonia emissions between methods when measuring in parallel after slurry application can be high: 32–46 % for IHF and wind tunnels (Scotto di Perta et al., 2019), 8–32 % for four aerodynamic flux gradient systems (Milford et al., 2009), and 1–7 % difference for bLS measured with two similar instruments at two different heights (Kamp et al., 2021). In addition, Vilms Pedersen et al. (2018) focused on the importance of plot size for bLS and compared methods also included in this study IHF, ZINST, bLS, and DTM (Vilms Pedersen et al., 2018). Calculating average cumulative emissions for the micrometeorological methods from the same plot size (20 m radius) showed 6–28 % relative difference for IHF, ZINST, and bLS and 41–76 % for DTM and wind tunnels compared to the average emission from micrometeorological methods (Vilms Pedersen et al., 2018). Another study measuring ammonia emissions after field application of organic fertilizer using IHF reported relative standard deviation of 23 % and 52 % among replicate plots (Misselbrook et al., 2005). Relaxed eddy accumulation measurements showed average fluxes 20–70 % lower than a gradient system taken as the reference (Hensen et al., 2009). Other studies focusing on evaluation of wind tunnels (WT) found that chamber configuration and design substantially affect the recovery of a known emissions within the chamber, but also that it is possible to achieve 100 % recovery (Loubet et al., 1999a; Pedersen et al., 2024). A recent study found that two different chamber designs resulted in relative differences in cumulative emissions of 43 % from the same field application (Pedersen et al., 2024). Controlled release experiments to evaluate the bLS model and filtering criteria found that it is possible to determine emission with recoveries close to 100 % and standard deviation among measurement intervals typically less than 20 % (Flesch et al., 2014, 2004; Gao et al., 2010, 2009; Häni et al., 2018; Lemes et al., 2023; McBain and Desjardins, 2005; Yang et al., 2016). Based on previous release experiments the bLS method can provide accurate measurements on average, but these comparisons do not account for error in TAN concentration in the slurry and application, i.e., errors in measuring application rate and errors in sampling and analysis of applied slurry, which would contribute to error in measured relative emission (emissions factors).

Because bias related to the measurement method varies among

research groups (Hafner et al., 2018) and even within categories of methods, an understanding of differences will require numerous comparisons that include multiple research groups. Based on the requirement of accurate emission estimates a closer look at measurement method differences is needed and is the focus of the present work.

The aim of the present work was to quantify error in ammonia emission measurements determined with methods commonly used after field application of slurry. Both bottom-up and top-down approaches can be used to estimate error (Possolo and Iyer, 2017). Although bottom-up approaches can be useful for estimation of random or systematic error, accurate estimation of error depends on accurate estimates of individual components, which can be difficult to make (Miller and Miller, 2018). Some of these estimates are subjective. More importantly, any systematic error, or bias, associated with a particular method, location, or experiment (or the distribution of this bias) is almost always unknown, and application of bottom-up approaches often omit a clear description of whether estimates of individual error sources include systematic components. These or related limitations probably contribute to a tendency for bottom-up uncertainty approaches in analytical chemistry to underestimate variability among laboratories (reproducibility standard deviation), which is itself already an underestimate of uncertainty (Thompson and Ellison, 2011). With the possibility of measuring an emission rate separately within many separate time intervals (thousands or more) using high-frequency measurement methods, the error propagation rules normally applied for random uncorrelated errors will provide vanishingly small—and implausible—estimates of overall uncertainty in total emission. This serves as a reminder of the likely importance of systematic errors, which are more difficult to estimate and therefore to include in bottom-up approaches. In contrast, top-down approaches include all unidentified biases based on a comparison of end results, thus does not rely on arbitrary estimates of individual error components. This work uses a top-down approach for estimation of measurement error based on application of multiple measurement methods in parallel by different research groups from different institutions in two field experiments.

The first experiment in Denmark (I-AU) used trailing hose application of slurry on bare arable land and the second experiment in the Netherlands (II-WUR) open slot injection on grassland. The following emission measurement methods were used: 1) the bLS method with a) CRDS, b) ALPHA samplers, and c) impingers for concentration measurement, 2) an open dynamic chamber method with Dräger tubes (DTM), 3) wind tunnels (WT) with CRDS, 4) IHF with impingers, and 5) off-site dynamic flux chambers with impingers (FC). Only two methods were used in both experiments (1a, bLS-CRDS and 3, WT); for the experiment conducted in Denmark (I-AU) 1a, 1b, 2, and 3 were used while 1a, 1c, 3, 4, and 5 were used in the experiment conducted in the Netherlands (II-WUR). Measurements of ammonia flux and cumulative emission made with these different methods were compared directly within each experiment. Additional quantification of differences in measurements from an estimate of "average" micrometeorological measurements was made by comparison to a semi-empirical emission model with parameter values determined from fitting to measurements made in about 600 field plots. The new emission measurements made in the present work were also used to evaluate the model and the underlying data set used for parameter estimation. This study is rare in including multiple emission measurement methods by different research groups in the same field trials. This design facilitates more realistic estimation of measurement error than typical studies employing a single method, or multiple methods applied by a single research group at a single location.

2. Materials and methods

Two experiments following slurry application were conducted to investigate ammonia emissions measured by different methods. One experiment was conducted at AU Viborg, Aarhus University (AU), Denmark, and one at Wageningen University and Research (WUR), the Netherlands. Different measurement methods and application techniques were used in the two experiments (Table 1).

2.1. Site descriptions

2.1.1. Field experiment I-AU

The experiment conducted in Denmark (I-AU) started August 20, 2021, and lasted for 7 days. Digested slurry was applied with trailing hoses (OD: 45 mm) that had 30 cm distance between the hoses. The driving speed of the tractor applying the slurry was approximately 7.5 km h^{-1}. The digested slurry was transferred to a storage tank approximately 3 weeks prior to the I-AU experiment. The digested slurry from the biogas plant at Aarhus University was mainly based on cattle manure, but also with other substrates (Table S1). The biogas plant consists of two sequential reactors with a retention time of 14 days at 51 °C and 40 days at 47 °C, giving a hydraulic retention time (HRT) of 50–55 days. The digested slurry was mixed prior to application.

A flat field with loamy sand was used and there was 7 cm of barley stubble remaining from a harvest that summer. Soil cores of 100 cm^3 in 0–5 cm were used to determine the dry bulk density and gravimetric water content. See Table 1 for soil properties. The plot size for the micrometeorological measurements was approximately 780 m^2 and WT measurements were conducted approximately 60 m west of the plot (Fig. 1).

2.1.2. Field experiment II-WUR

The experiment conducted in the Netherlands (II-WUR) started November 9, 2021, and lasted for 7 days. Cattle slurry was applied with shallow double disc injection (open slot injection) with a slot spacing of 17.5 cm in the WT experiment and 18.5 cm in the field experiment (bLS and IHF). The cattle slurry was from a local dairy farmer, and it was mixed prior to application.

Table 1
Overview of conditions, measurement methods, and slurry properties during the two experiments I-AU and II-WUR. Soil properties are shown with standard deviation ($n = 3$).

Experiment	I-AU	II-WUR
Application time, micrometeorological plot	20–08–2021 10:58	09–11–2021 10:15
Application method	Trailing hose	Disc (open slot) injection
Measurement methods	bLS-CRDS, WT, DTM, bLS-ALPHA	bLS-CRDS, WT, IHF, bLS-Impinger, FC
Slurry type	Digestate	Cattle
Application rate (tonne slurry ha^{-1})	35.9	bLS and IHF: 17.5 WT: 20.0 FC: 20.8
Application rate (kg TAN ha^{-1})	70	30 WT: 34.5 FC: 35.8
Slurry DM (%)	4.95	6.78
Slurry TAN (g N kg^{-1})	1.95	1.73
Slurry pH (laboratory)	7.9	7.7
Crop	Stubble	Grass
Stubble/Crop height (cm)	7	8
Soil type	Loamy sand	Sandy soil
Soil pH (1:1 water pH)	5.4 ± 0.2	6.7 ± 0.1
Dry bulk density of the soil	1.29 ± 0.17	0.98 ± 0.02
Gravimetric water content of the soil	0.21 ± 0.01 g^{-1}	0.49 ± 0.02 g^{-1}
Cumulative precipitation^{+} (mm)	0.6	5.0
Average temperature^{+*} (°C)	14.6	7.5
Average wind speed^{+*} (m s^{-1})	2.1	1.7
Air temperature at application (°C)	15.5	7.0

$^{+}$ Over 7 days (168 h) following slurry application. *Measured at 2 m height.

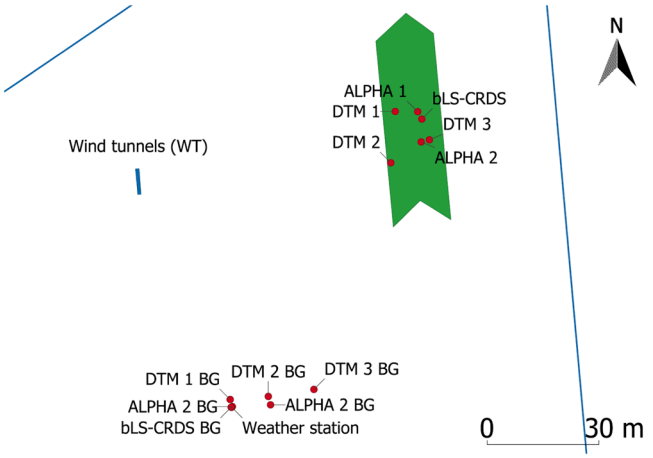

Fig. 1. Field layout during I-AU with position of weather station, background measurements used for the backward Lagrangian Stochastic model with cavity ring-down spectroscopy (bLS-CRDS), the Dräger Tube Method (DTM), and the backward Lagrangian Stochastic model with ALPHA samplers (bLS-ALPHA) and measurements inside the plot area for DTM, bLS-ALPHA, and bLS-CRDS. The blue area marks the area for the wind tunnels and the green area marks plot where slurry was applied. The blue line indicates the edge of the specific field.

A flat grass field with sandy soil and wet conditions with an average grass height of 8 cm was used. See Table 1 for soil properties. For the WT plots and FC soil samples, soil slots were made the day before the experiment started by a 3 m wide tractor-mounted experimental device with the same shallow injection equipment as used in the large micrometeorological plot. The plot size for the micrometeorological measurements was approximately circular with a radius of approximately 22.5 m (area of 1540 m^2) and WT measurements were conducted approximately 80 m southwest of the plot (Fig. 2). The plot was created by applying the slurry over a pre-marked area in 5 parallel passes that varied in length. The amount of applied slurry was measured by weighing the slurry tank before and after application. Undisturbed 14 cm deep soil samples, complete with intact grass, were excavated a day prior to the start of the experiment for use in the dynamic FC.

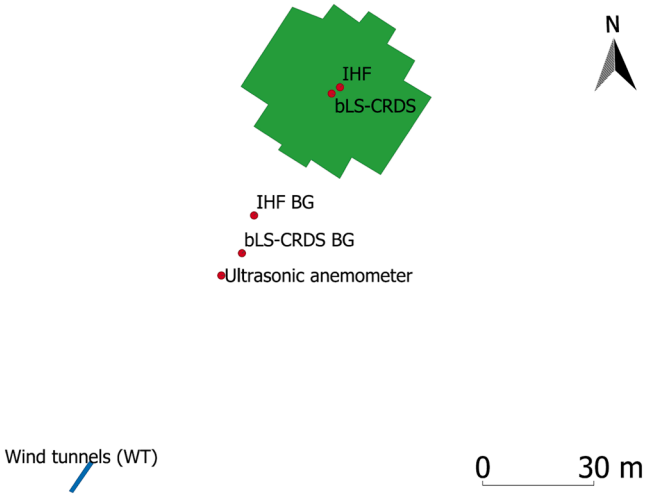

Fig. 2. Field layout during II-WUR with position of ultrasonic anemometer, background measurements used for the Integrated Horizontal Flux method (IHF) and the backward Lagrangian Stochastic model with cavity ring-down spectroscopy (bLS-CRDS) and measurements inside the plot area for IHF and bLS-CRDS. The blue area marks the area for the wind tunnels and the green area marks the plot where slurry was applied.

2.2. Measurement of emissions

The methods used were bLS with concentration measurement from CRDS, ALPHA samplers, or impingers (bLS-CRDS, bLS-ALPHA, and bLS-Impinger); IHF with concentration measurements from impingers; WT with concentration measurement from CRDS; DTM with Dräger tubes; and FC with impingers. There were inherent differences between the measurements, e.g., CRDS measures continuously giving a high time resolution while ALPHA samplers and impingers yield time-averaged concentrations over each exposure period. The bLS-CRDS and WT emission data from I-AU were previously presented by Hafner et al. (2024) along with two other experiments to compare these two methods using the ALFAM2 model.

2.2.1. Integrated horizontal flux (IHF)

The IHF method is a micrometeorological mass balance method used to determine emissions. Profile measurements of the wind speed and concentration are used to determine the vertical flux (Eq. (1)).

$$F_{IHF} = \frac{1}{x}\left[\int_{z_{0,ws}}^{z_p} \overline{u_{dw,z}} \cdot \overline{c_z}\, dz - \int_{z_{0,ws}}^{z_p} \overline{u_z} \cdot \overline{c_{uw,\,z}}\, dz\right] \quad (1)$$

In Eq. (1), F_{IHF} is the vertical flux (μg m^{-2} s^{-1}), the integral limit z_0 (m) is the height where the wind speed equals zero and $z_{p,WS}$ (m) is the height where the gas concentration equals the background level. The fetch length is denoted by x (m), $\overline{u}$ (m s^{-1}) and $\overline{c}$ (μg m^{-3}) are the mean values of wind speed and ammonia concentration at the height z (m), and subscript *uw* and *dw* denotes concentration measured up- and downwind, respectively (Ryden and McNeill, 1984). The data were analyzed according to Goedhart et al. (2020) using an exponential concentration model, which provides an overall better fit than the commonly used profile from Ryden and McNeill (1984).

Five minutes after slurry application to the first half of the plot, a mast supporting five impingers was placed in the center of the experimental plot. Measurements were done for a sequence of nine shifts after application of the slurry. The acid solutions in the impingers were collected and changed at 1, 3, 6, 23, 30, 47, 70 and 96 h after slurry application. The average wind speed was measured with cup anemometers (A100R, Vector Instruments, North Wales) at six heights: 0.24, 0.41, 0.86, 1.38, 2.39, and 3.57 m. The experiment employed five heights for concentration measurements within the source plot (0.25, 0.54, 1.04, 2.02, and 3.29 m) and background measurements at three heights (approximately 0.5, 1, and 2 m).

The impingers (acid traps) had a volume of 100 mL and were used to determine the ammonia concentration used for IHF. Furthermore, the ammonia concentrations measured with impingers were also used with bLS (see Section 2.2.2). The impingers trap ammonia in an acidic solution (20 mL of 0.05 M HNO_3) by pulling air through the glass impinger containing the acidic solution via a stainless-steel tube with a perforated Teflon cap using a suction pump (Thomas G045, Thomas by Gardner Denver, Monroe LA, USA) thereby trapping ammonia in the liquid phase. One pump was attached to one impinger and the flow rate per impinger was measured with flowmeters ("Rotameter", Platon, type B6D) and kept at 2–3 L min^{-1}. The flow rate was measured at the start and at the end of each sampling interval. The concentration of ammonia in the acidic solution was measured using spectrophotometry (colorimetry) to measure the NH_4^+ concentration in the acidic solutions.

2.2.2. The backward lagrangian stochastic (bLS) method

The bLS model operates backwards in time by modelling the transport of air based on the atmospheric conditions. The model (Flesch et al., 2004) was used with the R software package bLSmodelR (https://github.com/ChHaeni/bLSmodelR, v4.3, (Häni et al., 2018)) to estimate the ammonia flux in half hour intervals. The output of the bLS model is the concentration-to-emission ratio from the specific source (CE_{bLS}),

which is calculated based on the exact location of the source and sensors. Average interval flux was then calculated from Eq. (2).

$$F_{bLS} = \frac{(C_{downwind} - C_{upwind})}{CE_{bLS}} \quad (2)$$

In Eq. (2), F_{bLS} is the ammonia flux (mg s^{-1} m^{-2}), $C_{downwind}$ and C_{upwind} are ammonia concentrations (μg NH_3 m^{-3}) measured down- and upwind of the source, respectively, and CE_{bLS} (s m^{-1}) is the concentration-to-emission ratio obtained with the bLS model. The CE_{bLS} value was calculated for each averaging interval by simulating the backward air motion from the sensor. Inputs include the wind direction, friction velocity (u_*, m s^{-1}), atmospheric stability in the form of the Monin-Obuhkov length (L, m), the roughness length (z_0, m), and the standard deviation of the horizontal (σ_u, m s^{-1}), and vertical wind components (σ_v, m s^{-1}). In the two experiments, 100,000 trajectories were used to calculate the average flux for each half hour interval. Simulated trajectories that touch the ground inside the source area and their respective vertical velocity are used to calculate CE_{bLS}, as explained in detail by Häni et al. 2018. The performance of the bLS model is influenced by atmospheric conditions and filtering ensures that only data with high accuracy is included (Flesch et al., 2004). Intervals were discarded if either $u_* < 0.05$ m s^{-1}, $|L| < 2$ m, $z_0 > 0.1$ m, $\sigma_u / u_* > 4.5$, $\sigma_v / u_* > 4.5$, or $C_0 > 10$ (Bühler et al., 2021), where C_0 is the Kolmogorov constant of the Lagrangian structure function. To ensure accurate estimation of the overall cumulative loss of ammonia gap filling was employed to periods where data was removed. Although gap filling introduces some level of uncertainty, it is necessary to avoid underestimation caused by the removal of filtered data. In this study, linear interpolation was used as the method for gap filling. Most filtered (removed) data were from the night when lower wind speed and temperature, and therefore lower emissions normally occur.

The necessary inputs for the bLS model were obtained from an ultrasonic anemometer (WindMaster, Gill, Hampshire, UK) measuring the wind components at 16 Hz time resolution at 2 m. The wind components were used to calculate u_*, the wind speed and direction and L. The positions of instruments and slurry application area were measured with a GPS (I-AU: Trimble R10, Sunnyvale, California, USA; II-WUR: Topcon Hiper HR RTK GNSS, Livermore, California, USA).

Concentrations were measured continuously every 2 s with two CRDS instruments (model G2103 or G2509, Picarro Inc., Santa Clara, CA, USA). The instrument models have been evaluated for potential interference in an agricultural environment (Garcia et al., 2024; Kamp et al., 2019), while the model G2509 has been evaluated with the bLS method with release of know quantities of ammonia and methane (Yolanda Maria Lemes et al., 2023). With a sampling line, methane emission measured by bLS was 95 ± 8 % of the released amount, but only 82 ± 5 % for ammonia with the best sampling line when measuring some distance from the source. The difference shows evidence of deposition between the source and sensor. This problem was avoided in the present study because concentration was measured inside the source. The model G2509 instrument has been used to measure agricultural emissions with the bLS method (Lemes et al., 2022; Lemes et al., 2023b). One instrument measured inside the source and the other measured the background concentration. During I-AU, model G2509 measured inside the source, while model G2103 was used outside the source and at both positions during II-WUR. See Figs. 1 and 2 show the positions of the analyzers. The inlet height was 0.5 m in I-AU and 1.0 m in II-WUR. The comparison of these instruments is very important as the concentration differences were used directly to determine the emission rate with bLS. Therefore, the instruments were calibrated in the laboratory with ammonia standard gas (Air Liquide, Horsens, Denmark, 10 ppm NH_3), zero air, and a dynamic dilution system with mass flow controllers (Bronkhorst EL FLOW, Ruurlo, The Netherlands).

In the I-AU experiment, ALPHA samplers were used inside the large plot (2 sampling points) and background plot (2 sampling points). The ALPHA samplers were placed inside the plot immediately after slurry application at 1 m height. The samplers were manufactured by the UK Centre for Ecology & Hydrology (Tang et al., 2001). ALPHA sampler ammonia concentration measurements have been validated for atmospheric concentrations up to 25 ppb (Martin et al., 2019). In preparation before exposure in the field, the ALPHA sampling filters for sampling ammonia were coated with citric acid and the body of the samplers was assembled in the laboratory. Three samplers were exposed per sampling point. In addition, three transport blind samplers were carried to each sampler exposure date. Citric acid is recommended as an absorbent for temperate climates, so 12% citric acid in methanol was prepared and 55 μl was added to each filter, followed by drying and storage in a refrigerator until exposure. In the field the samplers were changed twice a day, in the morning and evening. To ensure that no particles from the membrane contaminated the filter during transport, the membrane cap with the PTFE membrane was removed and the sampler body was quickly sealed with a new lid. For analysis, the coated filters were extracted with 3 ml deionized water for at least one hour. The measurement of the extracts was carried out with an ammonia selective electrode (Thermo Scientific Orion Versa Star Pro-Electrochemistry Meters, Waltham, USA).The air concentration of ammonia (C_{ALPHA}, μg m^{-3}) was calculated from the adsorbed ammonia amount (m_e (μg) in the samples inside the plot and m_b (μg) in the background), and measured laboratory concentrations multiplied by the extraction volume (Eq. (3)) (Tang et al., 2001).

$$C_{ALPHA} = \frac{m_e - m_b}{V} \quad (3)$$

The effective volume of air (V, m^3 h^{-1}) sampled by the ALPHA sampler is given by stationary air layer within the sampler and is calculated as V in Eq. (3).

$$V = \frac{D \cdot A_{DTM} \cdot t}{L} \quad (4)$$

In Eq. (4), L (m) is the diffusion path length ($L = 0.006$ m), and A_{DTM} (m^2) is the cross-sectional area ($A_{DTM} = 3.46 \cdot 10^{-4}$ m^2) and D (m^2 s^{-1}) is the diffusion coefficient ($D = 2.09 \cdot 10^{-5}$ m^2 s^{-1} at 10 °C) of the gas for the time of exposure (t, h) (Tang et al., 2001).

The ALPHA samplers were changed after 7 h for the first period followed by changes every approximately 12 h before the last three periods that had exposure times from 18 to 24 h. The concentration determined with the ALPHA samplers in each period were used with the bLS method for that time interval, where inputs were averaged over the exposure time for all 18 intervals.

In the same way, the concentration determined with impingers used for IHF in II-WUR was also used to determine the flux using bLS in time intervals matching the exposure time of impingers for IHF (see Section 2.2.1). Mean and standard deviation for bLS-impinger was calculated from the emission estimates with bLS at each of the three lowest heights. The two highest positions were omitted because the concentrations measured were very close to the background level. To compare the bLS with impinger and bLS with CRDS, the concentration of CRDS was averaged to match the time intervals of IHF. Resulting estimates are referred to as bLS-CRDS avg.

2.2.3. Wind tunnels (WT)

The wind tunnel system consisted of nine WTs and online measurements of ammonia by a CRDS instrument model G2103 (Picarro Inc., Santa Clara, CA, USA). A detailed description of the system can be found in Pedersen et al. (2020). Of the nine WT, seven were used in I-AU and three in II-WUR.

Digestate and slurry application was done manually with a hose connected to a watering can. The predetermined volume of digestate or slurry was evenly distributed in three narrow bands at the soil surface in the WT frame to mimic trailing hose application in experiment I-AU and in the four pre-made disc injection slots in experiment II-WUR.

The WT consisted of stainless-steel chambers (25 cm height, 80 cm length, and 40 cm wide) with an open bottom. The tunnels were mounted on a frame, inserted into the soil, giving a plot area of 0.2 m^2. A fan (models SEAT 20 (tunnel 1) and SEAT 25 (tunnels 2–9), SEAT Ventilation, Verniolle, France) with a motor (MS 71B-B34 BUSCH, Kållered, Sweden) connected to a frequency converter (ATV12H037M2, Schneider Electric, Rueil-Malmaison, France) was used to control the airflow within the chamber. The air exchange rate (m^3 of air flow per m^3 chamber volume per time, AER (min^{-1})) was kept constant within each chamber throughout the experiments. Both experiments had three WTs with an air exchange rate of 25 min^{-1}, corresponding to a calculated average air velocity (longitudinal) of 0.33 m s^{-1}. For experiment I-AU four additional tunnels were included, two with an air exchange rate of 7 min^{-1} and two with an air exchange rate of 54 min^{-1}, corresponding to a calculated average air velocity of 0.1 and 0.7 m s^{-1}, respectively. From each tunnel and from three background measuring points evenly distributed between the tunnels air was drawn through a heated and insulated (ELSR-M-15–2-AO, SAN Electro Heat, Græsted, Denmark) PTFE tube (OD: 6.35 mm, ID: 4.75 mm) to a rotary valve (C46R, C45R-8140EUTA, VICI, Valco Instruments Co. Inc., Houston, TX, USA) controlled by the CRDS instrument. Air from the valve was analyzed by the CRDS instrument for 8 min at each valve position in order to ensure good recovery of the ammonia (Pedersen et al., 2020). The mean of the last 30 s of measurements per measurement cycle (8 min) was used for further calculations, as this period has been found to yield stable reading (Pedersen et al., 2020). Recovery of ammonia throughout the system was tested in the field prior to the experiments with a standard gas (NH_3 10.17 ± 0.31 mol-ppm for I-AU and NH_3 9.94±0.30 mol-ppm for II-WUR, Air Liquide), and was found to be minimal 98 % in both experiments. An average of the background measurements (n = 3) was subtracted for each measurement cycle before further calculations.

The flux (F_{WT}, mg m^{-2} min^{-1}) was calculated from the background corrected concentration of ammonia (C_{WT}, mg m^{-3}), the airflow in the emission chamber (q_{WT}, m^3 min^{-1}), and the area of soil surface covered by the tunnel (A_{tunnel}, m^2) (Eq. (5)).

$$F_{WT} = \frac{C_{WT} \cdot q_{WT}}{A_{tunnel}} \quad (5)$$

Cumulative emission was calculated from the flux using the trapezoidal rule. In experiment II-WUR, data was not recorded from 12.1 to 22 h after slurry application due to instrument error.

The effect of air exchange rate on emission was tested with measurements in I-AU by simple linear regression with relative 168 hour cumulative emission as the response variable and WT plot as the unit of analysis. The lm() and summary.lm() functions from the stats package in R v4.2.3 were used (R Core Team, 2023).

2.2.4. Dräger tube method (DTM)

The Dräger tube method (DTM) (Roelcke et al., 2002) used in I-AU is a quantitative dynamic chamber measurement method to obtain emissions under field conditions when combined with an empirical calibration for considering environmental factors on chamber measurements (Pacholski et al., 2006). The calibration approach was tested and validated in various studies by comparison with the micrometeorological measurements bLS and ZINST used with different concentration measurement methods (Gericke et al., 2011; Ni et al., 2015; Quakernack et al., 2012). The DTM system consisted of four stainless steel chambers with a diameter of 11.5 cm, which were connected with PTFE tubes. A portable electrical pump was used to draw air through an indicator tube. The ammonia concentration (ppm) of the air was displayed immediately by a color change on the indicator tube. The interior of the chambers was conical to avoid “dead zones”. Soil rings connect the soil and the chamber so that the soil was disturbed as minimally as possible by the measurements. Immediately after fertilization, the soil rings for the chambers were placed in the soil with the enclosed area (415 cm^2) completely covered by slurry. The measured emission was multiplied by the fraction of slurry covered area estimated from image analysis on drone pictures (Figure S8), assuming emission rate from bare soil was zero. Measurements with DTM were carried out five times throughout the day between 7am and 7pm to account for diurnal flux variations. It was measured inside the large plot (n = 3) and background plot (n = 3) with separate chamber sets to prevent contamination by carryover. An average of the background measurements was subtracted for each measurement before further calculations. Cumulative emission was calculated from the flux using the trapezoidal rule. Measurement raw data were converted to absolute emissions using the empirical calibration provided in Pacholski et al. (2006) mainly accounting for the effect of varying ambient wind speeds on the deviation of chamber measurements employing one single head space exchange from ambient turbulent ammonia transport processes (Eq. (6)).

$$\ln(F_{DTM}) = 0.444 \cdot \ln(F_{raw,DTM}) + 0.59 \cdot \ln(WS_{2m}) \quad (6)$$

Where F_{DTM} (kg N ha^{-1} h^{-1}) is the ammonia flux after calibration, $F_{raw,DTM}$ (kg N ha^{-1} h^{-1}) is the flux data obtained using one defined air exchange rate in the chamber head space, and WS_{2m} (m s^{-1}) is the wind speed at 2 m height.

2.2.5. Off-site dynamic flux chambers (FC)

Off-site dynamic flux chambers were used to measure ammonia emissions using a controlled air exchange rate. A known flow rate of ambient air was pulled through a closed PVC cylinder serving as the flux chamber. The flux (F_{FC}, mg m^{-2} min^{-1}) was calculated from the background corrected concentration of ammonia (C_{FC}, mg m^{-3}), the airflow in the flux chamber (q_{FC}, m^3 min^{-1}), and the area of soil surface (A_{FC}, m^2) (Eq. (7)).

$$F_{FC} = \frac{C_{FC} \cdot q_{FC}}{A_{FC}} \quad (7)$$

The set up of the dynamic flow chambers is described in detail by Ruijter et al. (2010). Buckets (volume approximately 10 L, diameter 0.26 m, height 0.21 m) were filled with an undisturbed grass sod layer of 0.14 m depth, see Section 2.1.2. The bucket was placed in the PVC cylinder, and a perforated lid was placed on top of the cylinder resulting in a headspace volume of approximately 4 L above the grass sod. Air entered the bucket through the perforated lid. The headspace air was withdrawn from a central hole in the lid by a vacuum pump (Thomas 617CD32, Thomas by Gardner Denver, Monroe LA, USA) and pulled through a glass impinger (acid trap) with a volume of 250 mL trapping the ammonia in an acidic solution (100 mL of 0.05 M HNO_3). The air flow rate was controlled to be 4 L min^{-1} by restriction with a critical orifice. The flow rate for each FC was checked at the start and at the end of the experiment with a volume flowmeter (DEFENDER 510, Mesa Labs, Colorado, USA). The air exchange rate (m^3 of air flow per m^3 chamber volume per time, AER (min^{-1})) was 1 min^{-1}. This flow rate was selected to approximately obtain a similar emission factor for shallow injection as generally measured with IHF in field experiments (Goedhart et al., 2020). Directly after manual application of a predetermined amount of slurry to the grass sod, with an amount matching the application rate in the field experiment (Table 1), the measurements were started. Measurements continued for 166 h, during which acid traps were replaced after approximately 1, 3, 6, 22, 30, 46, 70, 95, 119, 142, and 166 h. All emitted ammonia was trapped by the impinger, giving a direct amount of emission per measuring interval. Measurements were conducted simultaneously in quadruplicates, including two blank measurements of soil sods without slurry. The experimental set up was located outside under a cover to meet local weather conditions (temperature and relative humidity) approximately 300 m from the field location. The FC experiment was started at the same time as the field experiment, with all 4 replicates started within a 15 min period.

2.3. Estimation of measurement error

Because all measurement methods have some error and true emission from field-applied slurry is always unknown, emission measurements were compared to each other rather than to a reference value. Numerous factors undoubtedly contributed to differences in true emission in the two field trials, and it was impossible to estimate the contribution of all individual variables on emission. Here, our focus was on differences among measurement methods, which were initially explored by graphical comparison of flux dynamics over time and a numerical comparison of cumulative emissions. To estimate the relative magnitude of differences in total cumulative emission, the average of micrometeorological results (from bLS-CRDS and bLS-ALPHA in I-AU and bLS-CRDS, bLS-Impinger, and IHF in II-WUR) was taken as an estimate of the true emission.

Overall error in measurement of total emission includes contributions from numerous sources. Use of a particular method likely has an associated systematic error, which may differ among research groups because of method characteristics unique to that group, e.g., related to concentration measurement or data processing. This error probably also varies among specific field trials, because of interactions between accuracy and conditions (e.g., filtering of bLS results) or other effects that depend on time (e.g., instrument calibration between trials). This general model was used to conceptualize and ultimately estimate error in total cumulative emission:

$$x_{i,j,k} = y_i + m_{i,j} + \varepsilon_{i,j,k}, \quad (8)$$

where $x_{i,j,k}$ is the k^{th} replicate of total cumulative emission measured in a particular field trial i by a specific method/group j, y_i is true emission in trial i, $m_{i,j}$ is the systematic error associated with method/group j in field trial i, and $\varepsilon_{i,j,k}$ is remaining random "measurement error", which depends on the method (i), trial (j), and replicate (k). It was assumed that $m_{i,j}$ and $\varepsilon_{i,j,k}$ are random variables with a mean of zero but with a standard deviation that may vary among field trials. This model is an example of a simple random-effects model for hierarchical data, (e.g. Pinheiro and Bates, 2000, pp 7–8) with the addition of index i for field trial. And it is similar to the random effects laboratory effects model presented by Toman and Possolo (2009, Eq. (3)). The term $\varepsilon_{i,j,k}$ includes multiple sources of error and could be estimated by repetition of a single method by one research group in a single field trial (as in Häni et al. (2018) and Misselbrook et al. (2005), for example). Because true emission y_i is unknown, here it is taken as the mean of the different measurements, which is unlikely to be exactly true; therefore, systematic error may be underestimated. For chamber methods, which are generally not used to determine absolute emission, y_i is simply the overall average. In this framework the magnitude of an individual bias term $m_{i,j}$ is not particularly interesting or useful, but the standard deviation of m_i among the methods/groups provides useful information on the distribution of systematic error. When measurements are made without replication, as is common with micrometeorological approaches, it is the sum $m_{i,j} + \varepsilon_{i,j,k}$ that describes overall error.

Random-effects models were used to estimate the terms in Eq. (8). The lmer() function from the lme4 package (Bates et al., 2015) (v1.1–29) was used with the restricted maximum likelihood method, with measurement method as a single random effect and $\log_{10}$-transformed final cumulative emission (fraction of applied TAN) as the response variable. In this case, the between-method standard deviation of $m_{i,j}$ is an estimate of how systematic error varies among methods, while the residual standard deviation of $\varepsilon_{i,j,k}$ is an estimate of random error in measured emission present among replicates within a single trial. Separate models were fit for micrometeorological and enclosure results for each trial (4 models in total). For micrometeorological methods, only bLS-ALPHA in I-AU and bLS-impinger in II-WUR included replicates, so random error was effectively assumed to be identical for the other methods. In contrast, all enclosure methods included replication. The $\log_{10}$ transformation was used to focus on relative variability and avoid nonsensical predictions of negative cumulative emission. For simpler interpretation standard deviation estimates were back-transformed using $10^s - 1$, where s is the standard deviation in transformed units, but resulting estimates are only approximate.

2.4. Application of the ALFAM2 model

The ALFAM2 R package (v3.17, https://github.com/sashahafner/ALFAM2) (Hafner et al., 2021) was used in the R environment (v4.4.0) (R Core Team, 2023) to predict emission for these two field trials. The model is described in Hafner et al. (2019). Briefly, it predicts cumulative emission by closed-form integration of first-order loss from two lumped pools of slurry TAN: a "fast" pool that represents slurry TAN exposed to the atmosphere, and a "slow" pool that includes slurry TAN within soil pores or injection slots, or otherwise less available for emission (Fig. 3). The instantaneous emission rate is given by Eq. (9), where j is the ammonia flux (kg h^{-1} ha^{-1}), F is fast pool quantity of TAN (kg ha^{-1}), S is the slow pool quantity of TAN (kg ha^{-1}), and r_1 and r_3 are the first-order emission rate constants.

$$j = r_1 F + r_3 S \quad (9)$$

Initial partitioning of TAN between the two pools depends on application method and slurry dry matter, and TAN is continuously transferred from the fast to slow pool. Instantaneous transfer may occur after slurry application by incorporation into the soil by plowing or harrowing. These additional processes are shown in Fig. 3.

Model predictions were generated from application and weather data associated with the bLS-CRDS dataset (pmid 1936 & 1937) with half-hour time resolution (see note S17 in Supporting Information). The model is designed for application to discrete measurement intervals where weather is assumed to be constant. The latest default parameter set 2 was used (Hafner et al., 2021, 2024). Predictor variables that affect predicted emission were application method, application rate, slurry TAN, DM and pH, air temperature, wind speed, and precipitation rate. The parameter set was developed from micrometeorological measurements of emission, based on the assumption that they are the most accurate estimate of true emission.

3. Results

The fluxes obtained for the first 48 h of the two field experiments are shown in Figs. 4 and 5. The difference in application method and season contributed to differences in flux estimates between the two experiments. The fluxes were measured over a week, but most of the emission occurred within the first two days after application in both experiments (Tables 2 and 3).

The first field experiment (I-AU) was conducted in August during a period with little precipitation (Fig. 6) and an average temperature of 14.6 °C and wind speed of 2.1 m s^{-1} over the first 7 days after slurry application by trailing hose (Table 1). For the second field experiment conducted in November (II-WUR), the average temperature was 7.5 °C

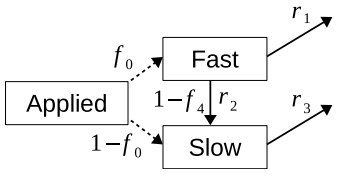

Fig. 3. General structure of the ALFAM2 model, following Hafner et al. (2019). Applied slurry total ammoniacal nitrogen (TAN) is immediately partitioned into fast and slow pools, as described by the f_0 parameter. TAN continually volatilizes and is transferred from the fast to slow pool based on first-order rate constants r_1, r_2, and r_3. The f_4 parameter quantifies instantaneous transfer by plowing or harrowing. See Hafner et al. (2019) for more details.

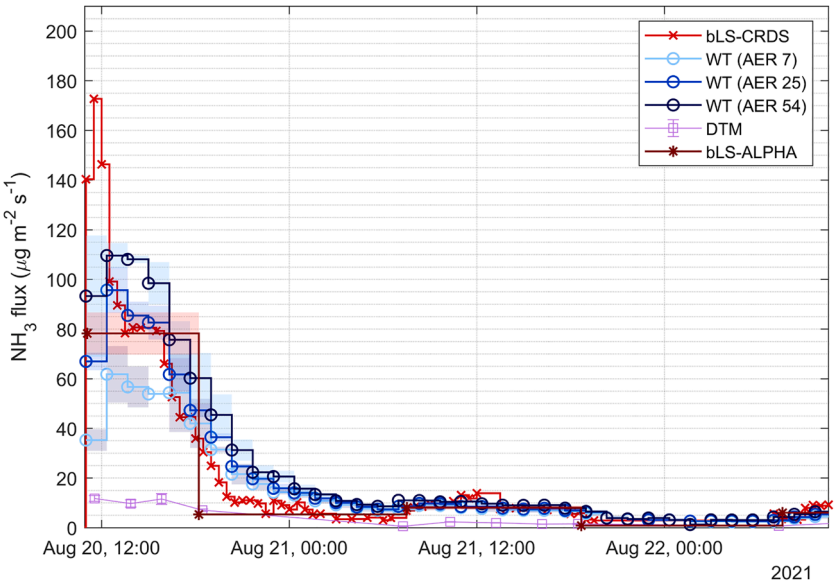

Fig. 4. Ammonia flux during I-AU for the first 48 h after application measured with the backward Lagrangian Stochastic model with cavity ring-down spectroscopy (bLS-CRDS), the Dräger tube method (DTM) ($n = 3$), wind tunnels (WT) with air exchange rates (AER) of 7 ($n = 2$), 25 ($n = 3$), and 54 ($n = 2$), and the backward Lagrangian Stochastic model with ALPHA samplers (bLS-ALPHA) ($n = 2$). The horizontal line represents the exposure or averaging period for the different methods, where the points mark the beginning of an interval. Shaded regions show ± 1 standard deviation for each interval. See Figure S2 for ammonia flux during the whole experiment duration (168 h).

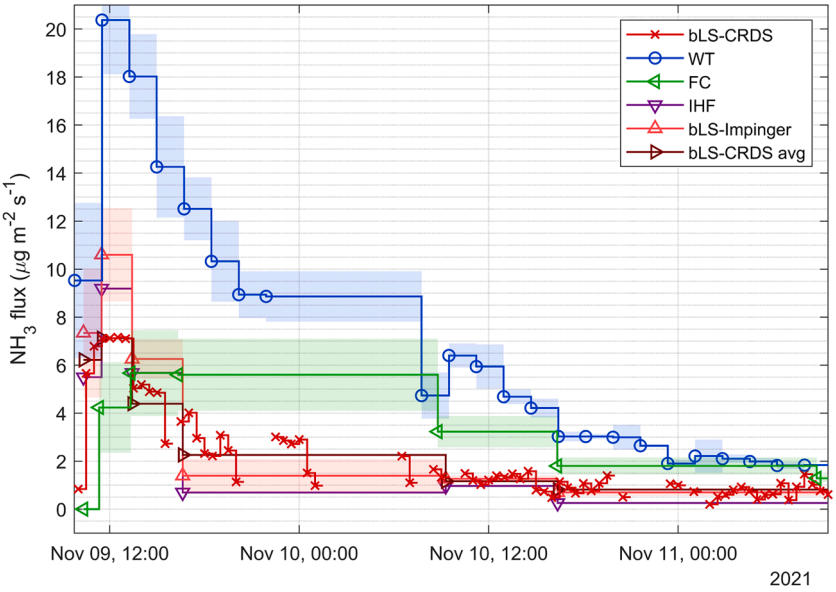

Fig. 5. Ammonia flux during II-WUR for the first 48 h after application measured with the Integrated Horizontal Flux method (IHF), the backward Lagrangian Stochastic model with impinger (bLS-Impinger), the backward Lagrangian Stochastic model with cavity ring-down spectroscopy time averaged to match IHF intervals (bLS-CRDS avg.), the backward Lagrangian Stochastic model with cavity ring-down spectroscopy (bLS-CRDS), flux chambers (FC) ($n = 4$), and wind tunnels (WT) ($n = 3$). The horizontal line represents the exposure or averaging interval for the different methods, where the points mark the beginning of an interval. Shaded regions show ± 1 standard deviation for each interval. See Figure S9 for ammonia flux during the whole experiment duration (168 h).

and wind speed 1.7 m s^{-1} over the first 7 days after slurry application by shallow injection (Table 1). Weather is shown in Figs. 6 and 7 for the two experiments.

3.1. *Field experiment I-AU*

The emission was highest immediately after slurry application, which was observed with all measuring methods (Fig. 4). However, the DTM estimates were much lower than all other methods on the first day, which affected cumulative emission substantially (Fig. 8, Table 2 and S15). After the first day, emissions obtained by DTM were much closer to the other methods. WT measurements included three different air exchange rates yielding three different initial emission rates; later the three converged into the same pattern. The highest emission was measured with the highest air exchange rate, leading to a clear positive and nearly linear effect of air exchange rate on cumulative 168 hour emission ($p = 0.0025$ from an F-test from regression analysis). This effect was expected and has been shown previously (Hafner et al., 2024). The bLS-ALPHA estimates were determined as averages over the exposure time, shown as the horizontal line in Fig. 4. With the lower time

Table 2
Cumulative emission (± 1 standard deviation for measurements with replicates) as the fraction of applied TAN in percentage (% of TAN) 24, 48, 72, 96, and 168 h after application in I-AU measured with the backward Lagrangian stochastic model with cavity ring-down spectroscopy (bLS-CRDS), the Dräger tube method (DTM) ($n = 3$), bLS-ALPHA ($n = 2$), and wind tunnels (WT) with air exchange rates (AER) of 7 ($n = 2$), 25 ($n = 3$), and 54 ($n = 2$), along with predictions from the ALFAM2 model (parameter set 2).

Hours	Cumulative emissions (% of TAN)						
	bLS-CRDS	DTM	bLS-ALPHA	WT (AER 7)	WT (AER 25)	WT (AER 54)	ALFAM2
24	33.5	8.3 ± 0.6	30.6 ± 2.0	25.3 ± 3.7	33.1 ± 1.0	40.2 ± 1.8	20.3
48	39.6	11.4 ± 0.8	33.8 ± 1.9	29.9 ± 4.5	38.1 ± 0.8	46.0 ± 1.7	21.5
72	44.4	13.4 ± 0.9	34.9 ± 1.9	32.6 ± 4.9	39.2 ± 0.8	49.1 ± 1.7	22.9
96	46.4	14.3 ± 1.0	35.7 ± 2.0	34.5 ± 5.2	42.9 ± 1.0	51.2 ± 1.7	24.2
168	49.8	15.6 ± 0.9	36.9 ± 1.7	37.2 ± 5.7	45.9 ± 1.1	54.5 ± 1.7	28.1

Table 3
Cumulative emission (± standard deviation for measurements with replicates) as the fraction of the total amount of applied TAN in percentage (% of TAN) 24, 48, 70, 96, and 168 h after application for II-WUR measured with the Integrated Horizontal Flux method (IHF), the backward Lagrangian Stochastic model with impinger (bLS-Impinger), the backward Lagrangian stochastic model with cavity ring-down spectroscopy time averaged to match IHF intervals (bLS-CRDS avg.), the backward Lagrangian stochastic model with cavity ring-down spectroscopy (bLS-CRDS), flux chambers (FC) ($n = 4$), and wind tunnels (WT) ($n = 3$), along with predictions from the ALFAM2 model (parameter set 2).

Hours	Cumulative emissions (% of TAN)						
	IHF	bLS-CRDS avg.	bLS-Impinger	bLS-CRDS	WT	FC	ALFAM2
24	5.4	7.2	7.2 ± 1.6	6.8	20.6 ± 1.8	11.1 ± 2.6	7.6
48	6.4	9.3	9.2 ± 1.9	8.9	26.8 ± 2.0	15.3 ± 3.2	10.4
70	8.0	10.8	11.4 ± 2.0	10.4	29.4 ± 2.0	17.5 ± 3.3	12.2
96	8.0	12.4	14.8 ± 2.3	12.0	31.9 ± 2.0	19.2 ± 3.5	13.9
168	–	–	–	12.9	35.6 ± 2.3	23.0 ± 3.7	17.9

resolution, early dynamics were not quantified, thus it was only possible to observe emissions starting at a level similar to the other methods before decreasing, and cumulative emission was more useful for comparison (Fig. 8).

Averaging the CRDS concentration measurements at the same time intervals as the ALPHA samplers shows that the average CRDS concentration tended to be higher than the ALPHA sampler concentrations in the first days when ammonia concentrations were highest (Figure S5). The CRDS inlet and ALPHA sampler 1 were placed close to each other, whereas ALPHA sampler 2 was placed farther south (Fig. 1), which influenced the concentration footprint area for each of the positions. This issue was accounted for with the bLS model that includes the geometry of the source and position of each sensor. The background concentrations measured with ALPHA samplers tended to be lower than CRDS measurements (Figure S6). Periods where measured ALPHA concentrations were close to zero for both background and plot measurements indicate that the measurements were close to the detection limit.

The bLS-ALPHA estimated fluxes from two different ALPHA sampler positions match well with each other as seen from both individual fluxes (Fig. 4) and the cumulative flux (Fig. 8). The difference in cumulative flux was mainly caused by the difference in the first interval, where ALPHA sampler 2 measured a higher emission. However, bLS-ALPHA provides generally lower fluxes compared to bLS-CRDS in high time resolution (Fig. 8) and for the CRDS fluxes averaged to match the exposure time of the ALPHA samplers (Fig. 9).

The ALFAM2 model predictions had the highest fluxes directly after application followed by a drop 1–2 h after application. The rapid decrease in the predicted fluxes consistently caused lower predicted total cumulative emission than measured by all methods except DTM (Table 2).

Random-effects model estimates of systematic error in measurement methods from between-method standard deviation for the two micrometeorological methods was 24 % as a relative value, with an estimate of 4.8 % for random error standard deviation among replicates from the residual term (0.092 and 0.020 before back-transformation). For enclosure methods, values were 75 % for between-method standard deviation and 7.6 % residual (0.24 and 0.03 before back-transformation)

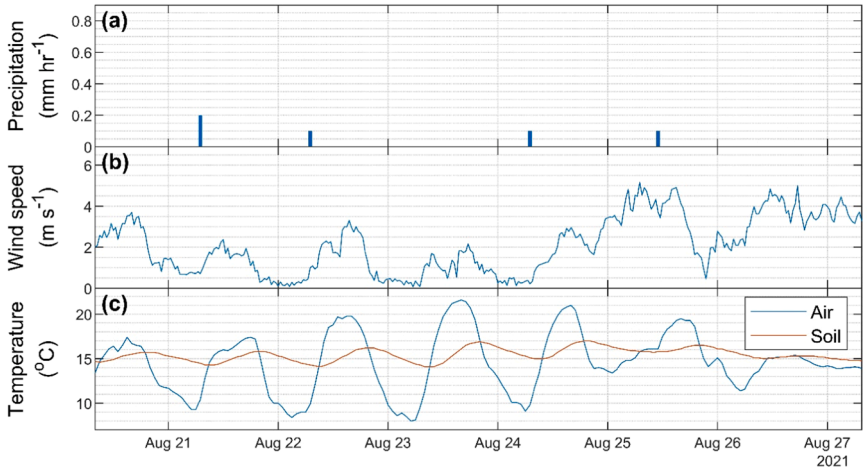

Fig. 6. Overview of (a) precipitation, (b) wind speed, and (c) air/soil temperature during I-AU. The air temperature and wind speed were measured at 2 m height and soil temperature at 10 cm depth.

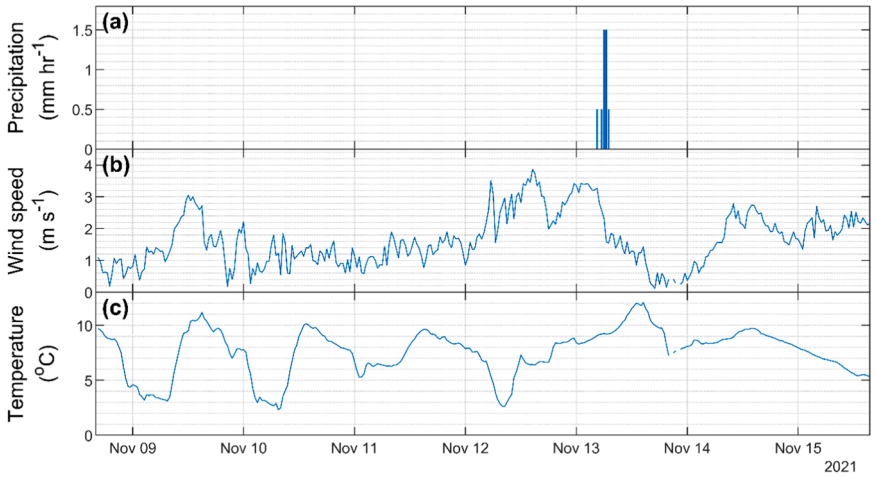

Fig. 7. Overview of (a) precipitation, (b) wind speed, and (c) air temperature during II-WUR. The air temperature and wind speed were measured at 2 m height.

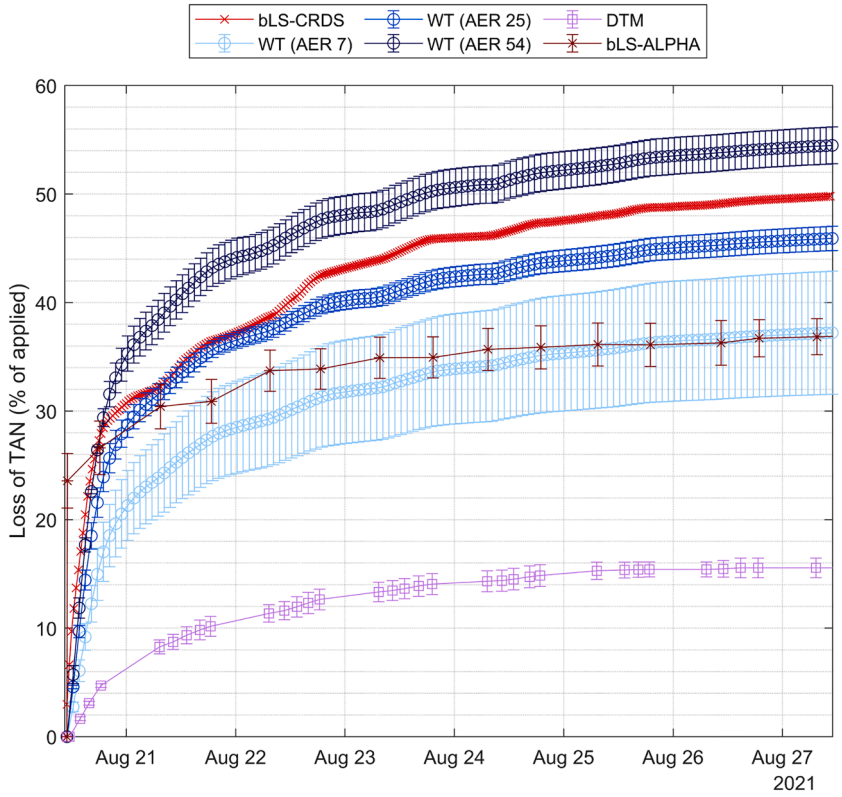

Fig. 8. Cumulative emission (± 1 standard deviation for measurements with replicates) as the fraction of applied TAN in percentage for I-AU measured with the backward Lagrangian Stochastic model with cavity ring-down spectroscopy (bLS-CRDS), the Dräger tube method (DTM) (n = 3), wind tunnels (WT) with air exchange rates (AER) of 7 (n = 2), 25 (n = 3), and 54 (n = 2), and the backward Lagrangian stochastic model with ALPHA samplers (bLS-ALPHA) (n = 2).

when results from three different wind tunnel AER were combined with DTM measurements. With only wind tunnel results, the between-method value was much lower, at 20 %, with a similar residual (0.08 and 0.03 before back-transformation).

3.2. *Field experiment II-WUR*

In the second experiment, all emission methods measured the highest flux within the first few hours after slurry application (Fig. 5, Table 3 and S16). However, maximum fluxes for bLS-CRDS, IHF, WT, and FC estimates were not immediately after slurry application, which was also observed for WT in I-AU.

Ammonia flux measured with IHF followed the pattern of the other methods, excluding WT, for the first 24 h. Later, IHF flux was lowest yielding the lowest cumulative emission estimates, however the flux for IHF and bLS was similar in the period 48–70 h after application. The ammonia concentration measured with the impingers was used for both IHF and bLS-Impinger emission estimates, where the cumulative emission from bLS-Impinger was higher compared to IHF (Fig. 10). Using average CRDS concentration that matches the exposure time for the impingers gives emissions (bLS-CRDS avg.) that are close to the bLS-impinger estimates. This was observed for both the individual periods (Fig. 11) and the cumulative emission (Fig. 10). The WT flux was much higher than other methods in the first two days after which the flux

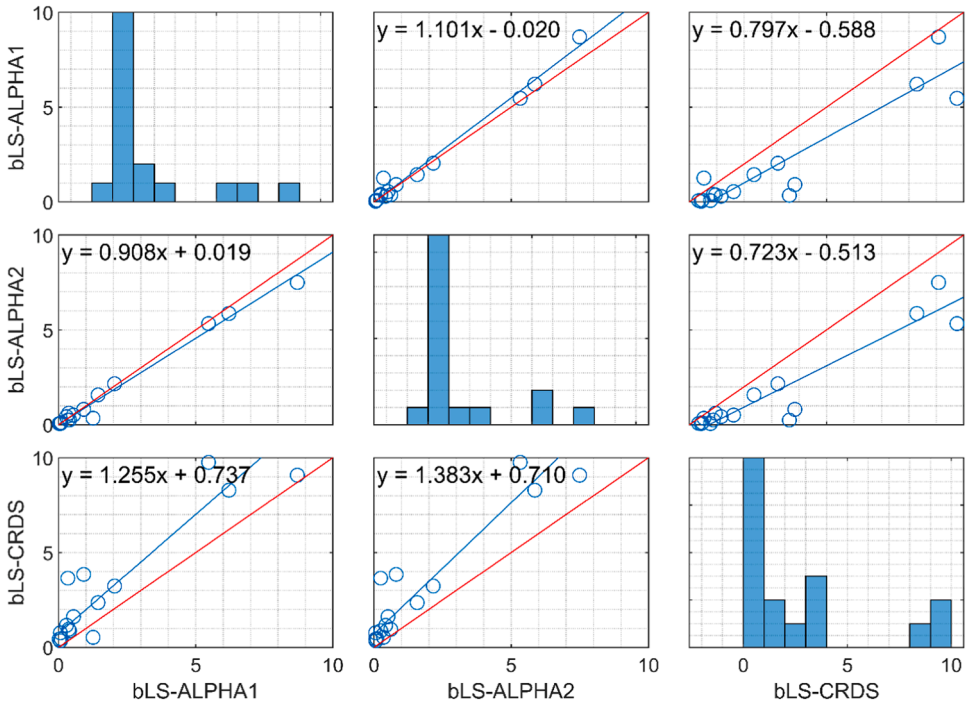

Fig. 9. Scatter plot with comparison of emissions for I-AU measured with the backward Lagrangian Stochastic model with ALPHA samplers (bLS-ALPHA1 and bLS-ALPHA2) and the backward Lagrangian Stochastic model with cavity ring-down spectroscopy (bLS-CRDS) and histograms for the distribution of fluxes for the same methods. Units for emissions in μg m^{-2} s^{-1} and histograms show counts on y-axis and emission bins (μg m^{-2} s^{-1}) on x-axis. The solid blue line represents the orthogonal regression line equal to the equation shown. The solid red line represents 1:1 slope. The first point was removed because of high influence. See Figure S3 for a plot with all data included.

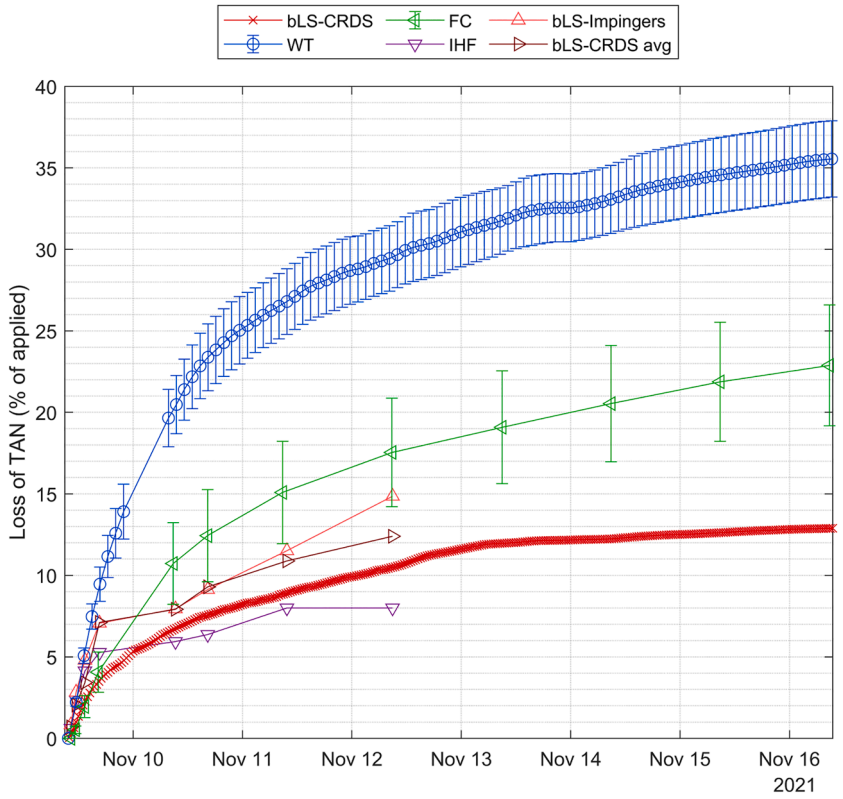

Fig. 10. Cumulative emission (± 1 standard deviation for measurements with replicates) as the fraction of the total amount of applied TAN for II-WUR measured with the Integrated Horizontal Flux method (IHF), the backward Lagrangian Stochastic model with impinger (bLS-Impinger), the backward Lagrangian Stochastic model with cavity ring-down spectroscopy time averaged to match IHF intervals (bLS-CRDS avg.), the backward Lagrangian Stochastic model with cavity ring-down spectroscopy (bLS-CRDS), flux chambers (FC) ($n = 4$), and wind tunnels (WT) ($n = 3$).

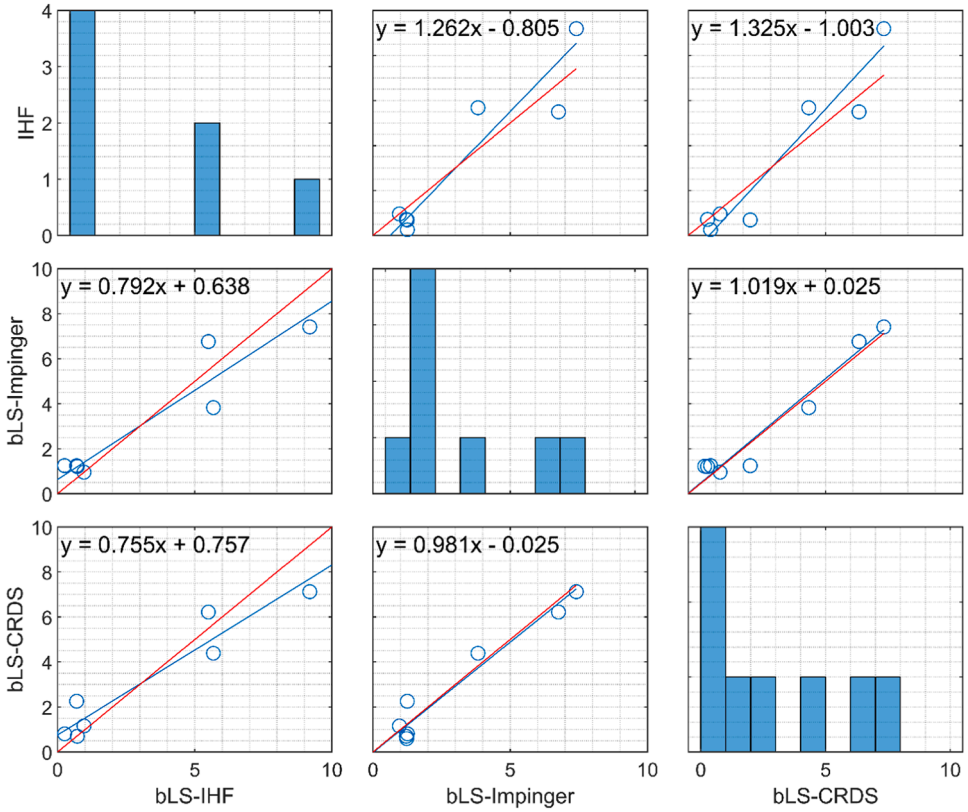

Fig. 11. Scatter plot with comparison of emissions for II-WUR measured with IHF, the backward Lagrangian Stochastic model with impinger (bLS-Impinger), and the backward Lagrangian Stochastic model with cavity ring-down spectroscopy time averaged to match IHF intervals (bLS-CRDS avg.) or histograms for the distribution of fluxes for the same methods. Units for emissions in μg m^{-2} s^{-1} and histograms show counts on y-axis and emission bins (μg m^{-2} s^{-1}) on x-axis. The solid blue line represents the orthogonal regression line equal to the equation shown. The solid red line represents 1:1 slope.

approached the same level as the other methods. WT emissions from 12.1 to 22 h after slurry application was interpolated due to lack of data. Cumulative WT emissions were at least twice as large as for the other methods mainly driven by the difference in the first two days (Fig. 5 and Table 3). FC emissions were between WT and micrometeorological results. FC emissions were generally higher than bLS results, caused by initial higher emissions during the first 48 h (Table 3).

Ammonia volatilization continued up to 96 h according to bLS-Impinger and bLS-CRDS results. Concentration measurements with impingers at five different heights were used for IHF. The measured concentration with CRDS was lower compared to impingers at the same height in the beginning and at the end of the experiment (Figure S11). The same was observed for the measured background concentration (Figure S12). For IHF a clear concentration profile was not observed in the last interval after 70 h (Figure S13), hence emission could not be calculated with IHF. However, the concentrations measured using the impingers were different from the background measurement, thus an emission was determined for the interval with bLS-Impinger. Therefore, the cumulative loss of TAN from IHF did not increase from 70 to 96 h, whereas the cumulative bLS-Impinger estimate in the same interval increased by 3.4 % of applied TAN (Table 3).

The fluxes predicted with the ALFAM2 model started at the same level as measured with bLS and IHF only with smaller differences in the first hours. The magnitude and pattern of the ALFAM2 fluxes were very similar to bLS-CRDS fluxes from 6 h after application until the end of the measurements (Figure S9). This is also seen as the cumulative emission calculated by the model was similar to measurements (Table 3). The difference between the nearest methods (bLS-CRDS and FC) and ALFAM2 predictions was small as a fraction of applied TAN (5 %), but the ALFAM2 result was 50 % higher than the average of the measurements by bLS-CRDS, bLS-Impinger, and IHF. The difference was about as large as the difference between IHF and bLS-CRDS results, expressed either way. Comparing FC and ALFAM2 shows that the difference was highest in the first 24 h and the fluxes were almost identical after 48 h.

Random-effects model estimates of systematic error in measurement methods from between-method standard deviation for the four micrometeorological methods was 25 % as a relative value, with an estimate of 17 % random error standard deviation from the residual term (0.097 and 0.069 prior to back-transformation). For enclosure methods, which included wind tunnels and flux chambers in this trial, equivalent values were 64 % for between-method standard deviation and 14 % for the residual standard deviation (prior to back-transformation, 0.22 and 0.056).

4. Discussion

4.1. Concentration measurements

The sampling frequency for CRDS was approximately 0.5 Hz, giving the possibility to observe the dynamic change of emissions in 30 min intervals for bLS-CRDS (Fig. 5). The exposure time for passive ALPHA samplers and impinger was short (7 h for ALPHA and 1–2 h for IHF) at the beginning of the experiments when emissions were high. Later, when ammonia concentrations were low, the exposure time was increased (>= 24 h) to increase sensitivity. Use of impingers and ALPHA samplers require manual handling in several steps including preparation, setup, collection, and laboratory analysis, likely contributing some systematic or random errors. For online measurements with CRDS, careful calibration is needed, especially when emission calculations are based on a measured concentration difference for bLS where there is a potential systematic bias between instruments. The use of ALPHA samplers for bLS with long averaging time was pushing the limits of the

applicability of the bLS model as the parameterization with Monin-Obukhov similarity theory (MOST) is only valid for short time intervals (Flesch et al., 2005b). The assumption of stationarity within averaging intervals of 12–24 h is not plausible, thus a bias will be introduced when using long averaging intervals within bLS. Just the contribution to the concentration measurement from the source is highly affected by changing wind directions for non-circular plots. This might be one factor that contributed to differences between bLS-ALPHA and bLS-CRDS emissions at later times. A higher time resolution of concentration sampling with ALPHA samplers in combination with circular plots would likely improve accuracy but is not always possible due to low sensitivity and constraints on equipment or field availability. This was partly overcome by the IHF impinger higher sampling interval and the use of a circular plot.

The bLS-CRDS, WT, and FC emission estimates increased from the first to the following intervals (Figs. 4 and 5) even though the highest emissions are commonly measured directly after application (Hafner et al., 2018; Huijsmans et al., 2003, 2001; Sintermann et al., 2011b). This response may be caused by a time lag in the measurement systems due to ammonia adsorption in tubing and the instrument, which potentially can cause underestimation of emission in the first intervals and overestimation in the following intervals. This effect did not apply to IHF in this experiment as the impingers were placed directly in the measuring tower without any tubing. Adsorption might also be a contributing factor to the very low fluxes obtained by the DTM in the first hours after slurry application (Fig. 4). The timing of the application also had some effect on the lag for bLS-CRDS as the slurry application started halfway through the first interval (Table 1).

4.2. Micrometeorological methods

Cumulative ammonia estimates for bLS-CRDS and IHF were relatively close after 24 h as a fraction of applied TAN (6.8 % for bLS and 5.4 % for IHF) and after 48 h (8.9 % for bLS and 6.4 % for IHF) (Table 3) in II-WUR. IHF equipped with impingers could not be used to estimate emissions after 70 h due to a lack of fit for the concentration profile model (Figure S13) even though bLS-Impinger and bLS-CRDS measured differences in ammonia concentrations compared to the background until 96 h with the same averaging intervals as the IHF (Table 3). An increase of 1.6 % of applied TAN in cumulative emissions from 70 to 96 h was seen for the bLS-CRDS avg. while an increase could not be estimated with IHF, likely making a small contribution to negative bias in IHF. Previously, IHF has been criticized as likely being positively biased, due in part to the contribution of horizontal turbulent diffusion, which can cause a systematic overestimation of 5–20 % depending on stability (Sintermann et al., 2012). The results presented here, where IHF estimates were lower than all other methods in II-WUR, do not support this suggestion. There are several different possibilities for fitting the profiles and a new method was proposed in 2020 (and applied in this study), which overall decreased emissions by a relative factor of 10 % for 160 Dutch experiments (Goedhart et al., 2020). The fitting procedure is a crucial step in the IHF analysis and therefore also a potential source of error (and an example of why method biases likely vary among research groups). The fitting procedure is closely related to the measured concentrations, and the individual contributions of profile determination and measured concentrations to observed differences among methods cannot be determined. However, bLS-Impinger and bLS-CRDS yield quite similar results, which (along with the lack of a profile from 70 to 96 h for IHF) could indicate that IHF estimation with the impingers was less sensitive to low emission rate. This could lead to lower estimation using IHF compared to bLS. However, there is an intrinsic distinction between IHF, which directly measures concentration and wind profiles from multiple heights within the boundary layer, and the bLS method that assumes that the wind profile can be based on the application of MOST by utilization of measurements at a single height and applies similarity relationships. The accuracy of the model is dependent on the accuracy of MOST-based description of the atmosphere; thus, some level of uncertainty is introduced with this assumption and reliance on the validity of MOST (Flesch et al., 2005a). This is the reason for filtering based on atmospheric conditions as the filtering removes periods with more extreme conditions where the assumptions are more likely to be violated (Flesch et al., 2014, 2005b). The filtering process of bLS-CRDS introduces a potential bias on cumulative emission with linear interpolation between remaining fluxes. Most removed data were from nighttime measurements where flux was lowest (Fig. 5), thus overestimation is possible. In addition, wind profiles measured for the application of the IHF indicated that assumption of the MOST were met by the experimental conditions because the wind profiles exhibit patterns as expected in all intervals (Figure S13).

4.3. Enclosure methods

Using different air exchange rates with WTs yielded significantly different flux levels and cumulative emissions in I-AU, highlighting the importance of considering air exchange rate for both experimental design and interpretation of enclosure results. While it may be possible to approximate open-air emission using chambers with an appropriate fixed value for air exchange rate, determining emission dynamics and effects of weather during a trial is more difficult. WT with AER = 25 min^{-1} and bLS-CRDS were measured in both experiments, and in I-AU AER = 25 min^{-1} yielded only slightly lower cumulative emissions compared to bLS-CRDS, but the same air exchange rate in II-WUR provided higher cumulative emissions compared to bLS-CRDS. Between the two enclosure methods in II-WUR (FC and WT) large differences were observed (Fig. 5), most likely caused by the much higher air exchange rate (25 min^{-1}) of the WT compared to FC (1 min^{-1}).

In II-WUR, the WT flux measurements and cumulative emissions were up to 3 times higher than the other methods (Figs. 5 and 10). Especially the first two days, the WT flux was much higher, which may be caused by handheld slurry application in one-day-old slots, the oasis effect, and a larger wind speed gradient close to the surface and higher turbulence within the enclosures (Loubet et al., 1999a, 1999b). In addition, the low open-air wind speed during this experiment (average of 1.7 m s^{-1}, Table 1) would tend to exacerbate the discrepancy between enclosure methods and micrometeorological methods. For WT, it has been shown that increased wind velocities increase ammonia emission (Saha et al., 2010; Sommer and Misselbrook, 2016). In enclosure methods it is common to select high air exchange rates to ensure mixing and minimize effects of variation in air flow (Cole et al., 2007; Parker et al., 2013), probably decreasing air-side resistance substantially compared to open-air conditions. For FC, the AER was relatively low compared to WT and mixing of the air was ensured by including multiple (24) inlets.

During the entire measurement period, cumulative emissions from the WT and FC methods showed a continuous increase (Fig. 10). In contrast, the emissions from the bLS-CRDS reached a plateau after approximately 96 h. This response was not observed in I-AU and is likely related to the rainfall at that time during II-WUR (Fig. 8).

Earlier work has shown how WT may under- or overestimate ammonia loss by changing air flow above the soil surface (Hafner et al., 2024; Sommer and Misselbrook, 2016). Considering this along with the results from the present study, enclosure methods should primarily be used for studying relative differences rather than providing absolute emission values. But it is still uncertain whether the effect of enclosure methods on absolute emissions may bias measured relative differences observed by enclosure methods between treatments. The air exchange rate of the FC was selected to match total emissions after shallow injection of slurry determined with IHF in previous experiments. Total emissions measured with the FC were in fact closer to the micrometeorological results than WT measurements were in this experiment with low emissions.

4.4. Dräger tube method (DTM)

The DTM measurements had the lowest emissions of all methods in I-AU with cumulative emissions less than half of bLS-ALPHA and less than one-third of bLS-CRDS and one-half to one-third of WT results, (depending on the air exchange rate in the WT). The largest differences in flux were found in the first 24 h of after slurry application, whereas DTM results were similar to the other methods later on (Fig. 4). DTM cumulative emissions were 64 % lower than average micrometeorological cumulative emission, which is close to the difference of 66 % observed by Vilms Pedersen et. (2018) for DTM compared to the average emission measured using micrometeorological methods.

The DTM method provides spot samples in time, which were measured during daytime when emission is expected to be highest as the highest temperatures and wind speeds were seen during daytime. Although measurements in the morning and in the evening are connected to lower temperatures and wind speeds than during the day, overestimation with DTM would be expected due to low sampling coverage of nighttime emission.

The spatial representativeness or extrapolation of the small-scale measurements can be considered one of the major drawbacks of this method for slurry application compared to mineral fertilizer application, where the fertilizers can be precisely applied in the area covered by the chambers. The use of four chambers with a small surface area (11.5 cm diameter) with 3 replicates on the plot is assumed to account for spatial variations in slurry application and heterogeneity. Spatial variation and heterogeneity are difficult to assess, but the low standard deviation for DTM in this experiment (Table 2) confirms variability was generally low between the three different DTM locations. It can only be speculated whether this is sufficient to account for the full-scale application heterogeneity in this experiment. The DTM chambers were placed fully over the slurry bands (Figure S7) and the emissions were corrected according to the slurry covered surface area, which was difficult to assess (Figure S8). Additionally, the concentration measured with the Dräger tubes were read manually on the tube from a colored gradient, which was as a source of random or systematic error.

Another source of error may be the empirical calibration approach to estimate absolute (open air) emission from chamber measurements (Section 2.2.4). The calibration is based on a comparison of DTM chamber to IHF measurements and depends on the measured wind speed. In previous comparative measurements of ammonia losses from surface-applied slurry and urea measured with the calibrated DTM were in close agreement to measurements with bLS (Gericke et al., 2011; Quakernack et al., 2012). However, another study only found a good agreement between DTM and bLS for mineral fertilizer whereas DTM yielded 44–70 % lower cumulative loss than bLS for pig slurry and digestate (Ni et al., 2015). It is possible that the assumption that the ratio between open-air and DTM flux varies (only) with wind speed is not correct, potentially explaining the variable performance of DTM. Considering the differences found in this present study, use of the DTM method for measurements of absolute ammonia emissions after slurry application should only be used after careful consideration as the emission is unevenly distributed and it is questionable if the small area of the DTM can account for this heterogeneity. DTM should be thoroughly tested and validated before using the method for slurry application as also indicated in another recent study (ten Huf and Olfs, 2023).

4.5. Effect of slurry application method and climate

Measured emissions were much higher for I-AU than II-WUR, which is clearly seen in cumulative emissions (Tables 2 and 3, Figs. 8 and 10). The micrometeorological methods showed 35–50 % loss of TAN over 168 h following trailing hose application in I-AU. Following open slot injection in II-WUR, only 8–13 % loss of TAN was observed with micrometeorological methods over 168 h. Several factors likely contributed to this difference between the two experiments: difference in application technique with trailing hose and shallow injection, different temperatures during application, and different slurry type and pH. Slurry injection has been shown to decrease ammonia emissions after field application as there is a reduced slurry covered surface area from where emissions can occur and a presumed higher degree of infiltration (Huijsmans et al., 2018, 2001; Webb et al., 2010). Ammonia emission increases with temperature (Huijsmans et al., 2018, 2003, 2001; Pedersen et al., 2021; Sommer et al., 2003). Thus, the lower temperature and slurry injection are expected to have caused the lower emissions for II-WUR. On the other hand, ammonia emission normally increases with wind speed, which was higher, on average, for II-WUR (Table 1), but the effect on injected slurry appeared to be of minor importance as the windspeed effect is lower for shallow injection (Huijsmans et al., 2018). Two different slurry types were used in the two experiments with digestate in I-AU and cattle slurry in II-WUR. The higher pH for the slurry in I-AU (Table 1) may also have contributed to higher emission (Fangueiro et al., 2015; Pedersen and Hafner, 2023), but the difference (0.2 pH units) is smaller than changes that have been measured in the same sample during storage (Hafner et al., 2018).

Rainfall may also reduce emission (Kamp et al., 2021), presumably due to dilution and transport of TAN downward away from the surface. Most precipitation occurred during II-WUR during one larger rainfall event four days after application giving 5.0 mm precipitation in total, whereas I-AU only had 0.6 mm precipitation in total. The rainfall could also be an explanatory factor for the lower emissions during II-WUR; however, as the rainfall occurred four days after application, it is most likely that it is of minor importance to the overall emissions with most volatilization within the 48 h as shown in Sections 3.1 and 3.2. The IHF measurements were stopped before the rainfall.

Slurry application was manual for WT and FC, unlike the other methods, and therefore any differences in emission measured with these two methods also included effects of slurry application. Plot placement for these methods was within the fields or with soil from the field used for the other methods, and therefore soil differences were likely of minimal importance. In the large plot with machine application in II-WUR, all the slurry was contained within the slots after application whereas handheld application in the WT setup resulted in contamination of the surface outside the slots (Figure S14). The slurry covered surface area was therefore higher inside the WT compared to the large plot. The slot probably collapsed somewhat before the slurry was applied the following day, thus injection was not adequately mimicked for the handheld application inside WT. It may have contributed to the dissimilarity between relative differences in cumulative emission after trailing hose application in I-AU and injection in II-WUR measured with bLS (injection was 74 % lower than trailing hose) and WT (22 % lower). This indicates that handheld slurry application is most suitable for application with no or minor interaction between the slurry application equipment and the soil i.e., it is easier to mimic trailing hose application with handheld application. The slightly larger application rate used inside the WT with 20.0 tonne ha^{-1} compared to 17.5 tonne ha^{-1} in the large plot was not expected to have any effect on emissions for shallow injection.

4.6. Ammonia emission measurement error

Observed variability in cumulative ammonia emission measured in different field trials under similar conditions is some combination of true differences in emission and measurement error, the latter including both systematic and random components. Classifying a particular source of error as systematic or random is not always straightforward (Possolo and Iyer, 2017, p 20). A particular measuring method may have a systematic error (bias) that persists across research groups, but errors related to location, time, experiment, or research group may be as important and may be considered random or systematic depending on the unit of analysis. The experimental design used in the present work eliminated differences in true emission for the methods used in parallel at the field

scale: bLS, IHF, and DTM methods. But the experimental design did not allow for complete partitioning of observed variability into different sources of error. The residual term from the random-effects model is an estimate of random error among replicates within a single experiment but is based only on those methods that were replicated (bLS-ALPHA and bLS-impinger). Systematic differences between methods within an experiment were estimated by the between-methods standard deviation, but it is not possible to determine whether errors are associated solely with methods, research groups, experiments, or some combination. Adding to the complexity of the problem, there are multiple possible mechanisms driving the observed differences, including error in concentration measurements, air flow measurements, or emission calculations and associated assumptions. Still, the error estimates are useful, and the limited partitioning is consistent with previous work, as described below.

The use of different concentration measurement methods to estimate emissions with the same method (e.g. bLS) provides a means of separating contributions of these different sources of error, although only for comparisons between bLS-CRDS, bLS-ALPHA, and bLS-Impinger, which differed in concentration measuring method only. The differences in bLS results (e.g., difference of 13 % of applied TAN between bLS-CRDS and bLS-ALPHA in I-AU and 2.8 % of applied TAN between bLS methods in II-WUR after 96 h) highlight the critical role of concentration measurements when determining emissions.

It can be concluded that errors in micrometeorological measurement of cumulative ammonia emission could be at least as large as 14 % of applied TAN, which was the maximum difference between bLS-ALPHA compared to bLS-CRDS in I-AU). With low emission, such as for slurry injection, relative measurement error could be quite high; in II-WUR the difference between IHF and bLS-Impinger results was less than 7 % of applied TAN, but with low emissions in this experiment this relative difference is 57 % of the average of the micrometeorological measurements. Random-effects model results provide a convenient quantitative summary of likely error in emission measurements. The $\log_{10}$ transformation used in that analysis (Section 2.3) implies an assumption of constant relative error, which is supported by the similarity in relative error estimates in the two experiments. For micrometeorological methods applied without replication within a trial ($n = 1$), residual and between-method standard deviation can be combined by adding in quadrature (Taylor, 1982, p 54) to estimate relative uncertainty in the overall emission measurement. With this approach the field trials provide an estimate of 24 and 31 % of the measured value (0.094 and 0.12 with $\log_{10}$ transformation, or about 0.1). Using twice the standard error estimate gives a confidence interval in a typical measurement of cumulative emission of about 60 to 160 % of the measured value ($10^{\pm 0.2}$). (This range is not symmetrical because of the transformation.)

Random error among replicates has been quantified in previous work and can be compared to results from the random-effects models. The 23 % coefficient of variation found among 3 replicate IHF plots by Misselbrook et al. (2005) suggests that random error is actually underestimated by the random-effects model results (at least in experiment I-AU), that the more current measurement methods used in the present work have better precision, or that other sources of random error not included in the replicates used in the present work (such as error in TAN application rate) are important. The measured variability among replicates reported by Häni et al. (2016) for bLS (15 % standard deviation) and IHF (10 %) were closer to the values estimated in the present work (7.6 % in I-AU and 17 % in II-WUR), perhaps more accurately reflecting the newer methods used in the present work.

Previous bottom-up error estimates aimed at estimating random error are also similar to the estimates provided by the random-effects models. The estimated total relative error in cumulative ammonia emission measurements (presumably an estimate of standard deviation of measured emission) from urine patches was 8 % in best cases and with a mean relative error of 12–16 % with the largest concentration differences using bLS while the mean relative error was 10 % for IHF (Laubach et al., 2012). In the analysis for bLS, it was assumed that wind speed error (~1 %) was negligible compared to horizontal flux error (~5 %) and with a random error of 6 % for the 50,000 trajectories used. In the present study 100,000 trajectories were used, which will decrease the stochastic error of the bLS model. Another study assumed a stochastic error of 10 % on the model result and a constant error on the background concentration of 0.5 μg m^{-3} (Häni et al., 2016). The error for bLS measurements in individual intervals can exceed 100 % in cases with low concentrations differences (Laubach et al., 2012), which highlights that the concentration difference is a key element for the error of the bLS method.

Variability among replicates and typical bottom-up error estimates do not include any systematic error, which is generally assumed to be negligible but may in fact be more important than random error; random-effects model estimates of systematic error from both I-AU and II-WUR were around 25 % (standard deviation). Measurements of ammonia emission from urea by IHF, ZINST, and bLS varied with a standard deviation of 10 % and 48 % in two field trials (Vilms Pedersen et al., 2018). Perhaps importantly, the different methods applied in these earlier studies were done by a single research group, so variability may be lower than among measurements made by different groups. These results highlight the importance of direct comparisons of emission measured with different methods by different research groups, which facilitate a realistic assessment of overall error that simple replication and bottom-up approaches cannot. Estimating bottom-up errors for bLS-CRDS would lead to low standard errors on concentration estimates as >1000 concentration measurements were averaged in each half hour time interval. Thus, bottom-up estimates of errors would rely on assumptions on the stochastic error (e.g. 5–10 %) or unmeasurable concentration errors and will not provide more information on errors unaccounted for.

Interestingly, systematic error estimates made in the present work tend to be larger than what some controlled release experiments have shown. In controlled release experiments, the bLS model has been tested for ammonia with open path instruments giving recoveries ranging from 0.69 to 0.91 when deposition between the sensor and the source was not accounted for and standard deviations depending on measurement position ranging 0.07 to 0.19 with the highest uncertainties observed with measurements farthest away for the source (Häni et al., 2018; Lemes et al., 2023). In this study, the measurements were made inside the source eliminating the effect of deposition to the non-emitting area between the sensor and the source. Using chemically inert methane for which deposition does not occur, release experiments have shown recoveries close to 100 % with standard deviation among replicates <20 % when proper filtering has been applied, e.g., Harper et al. (2010) found a standard deviation of 5 % among the recoveries from 9 different studies using releasing inert tracer gases (either CH_4, CO_2, or SF_6).

Although the estimate of systematic and therefore overall error in micrometeorological measurements from the random-effects models is not small, it is supported by the emission measurements compiled in the ALFAM2 database. An analysis of those values from more than 400 field plots generated by 13 different research groups actually showed a substantially larger value for the systematic component associated with individual research groups, with a standard deviation of 0.3 in $\log_{10}$-transformed units (Hafner et al., 2018), compared to around 0.1 in the present work. This larger value could be taken as evidence of even larger systematic error than the present comparisons show, but it is likely that a large fraction of the differences observed in the earlier work were caused by true differences in emission confounded with research groups, e.g., related to location or slurry characteristic effects not completely represented by model predictor variables such as air temperature or dry matter.

Replication is one strategy for reducing uncertainty in micrometeorological results by improving precision, but replication does not reduce systematic error in measurement methods (quantified by between-method standard deviation here). The micrometeorological results in

II-WUR with a high residual standard deviation imply that this strategy will somewhat improve results, while the lower value in I-AU does not. All these estimates are clearly imperfect. They are based on a limited number of methods, some of which were closely related, including bLS-Impinger and bLS-CRDS. It is possible that multiple methods have similar biases. Furthermore, the estimates of between-method standard deviation from these models are really an estimate of systematic error variability, not its magnitude per se (because it is necessary to assume y_i is the mean from all methods, and $m_{i,j}$ has a mean of zero; see Section 2.3). Both of these considerations imply that true systematic error is probably higher than between-method standard deviation indicates. Lastly, replicates were not available for all methods, and do not include all possible sources of random error where available, so partitioning between-method and residual error is tenuous, although this would not affect the total error and therefore has no impact when replication is lacking ($n = 1$).

The above discussion is focused on error estimates based on comparison of multiple methods simultaneously. Some insights can also come from comparing individual methods. In I-AU the largest relative difference among micrometeorological results was 30 % between bLS-CRDS and bLS-ALPHA, but IHF was not included in I-AU. These differences are comparable to the 20–70 % observed earlier between the aerodynamic gradient method and relaxed eddy accumulation (Hensen et al., 2009; Misselbrook et al., 2005).

Variability among different enclosure methods was clearly higher than micrometeorological methods in this study, and effects of changing wind tunnel AER was less important than differences among enclosure types, which could still be related to air flow. Because enclosure methods are not typically used for estimation of absolute emission, this result does not necessarily indicate a problem. Estimates of random error among replicates (the residual term) were low (7–14 % as a relative value), reflecting the low standard deviation values shown in Tables 2 and 3. Coupled with the relative ease of replication, this result highlights the utility of enclosure methods in comparisons, for example of application methods or slurry characteristics. Numerous studies demonstrate this use (Bhandral et al., 2009; Kai et al., 2008; Rochette et al., 2008). Because relative effects can depend on absolute emission (Hafner et al., 2024), it is logical to aim at designing and operating enclosure systems to approach micrometeorological results, including adjustment of flow rates as with the flux chamber and wind tunnel systems used in the present work. For comparisons, care should be taken to control other variables that are known to affect emission. Comparisons across multiple field trials risk inaccurate conclusions. Limitations imposed by the system also need to be considered. Slurry application is a good example from the present study. Handheld slurry application in WT II-WUR that poorly represented the successful injection carried out by full-scale equipment may have contributed to the difference between the only two methods applied in both trials when comparing the two trials the bLS-CRDS results showed 74 % lower emission after open slot injection in II-WUR, while the difference was only 22 % in wind tunnel results (AER 25).

4.7. ALFAM2 model

The ALFAM2 model with default parameter values provides estimates of emission for the two trials that might be expected under average conditions. Comparisons between model predictions and measured emission therefore provide further evidence that the differences observed here between different measurements methods are not unusual. In I-AU, a difference between the model and the bLS results of 9 and 22 % of applied TAN encompass average model error of 15 % of applied TAN (Hafner et al., 2021). Differences between average micrometeorological results and the model in II-WUR were smaller: 3–10 % of applied TAN, while average model error for open slot injection was 10 % (Hafner et al., 2021). Together these results are consistent with the conclusion that measurement error is a major part of the observed differences among emission measurements.

Undoubtedly the default set 2 parameter values for the ALFAM2 model do not exactly represent average global results, and the high-resolution measurements presented in the present study present an opportunity to carefully critique the model and parameter set. Parameter values for the ALFAM2 model are based on fitting to emission measurements from about 600 field plots. Any measurement errors present carry through to model parameter values. The structure of the model and the resulting predicted emission trajectory is based on comparison to measurements from hundreds of field plots. As discussed above, variability among emission measurements is often large. For all these reasons, it would not be reasonable to revise the ALFAM2 model based on results from only the two field experiments presented here. However, poor model performance in predicting emission dynamics for these experiments with multiple measurement methods can highlight model limitations that might be addressed in the future. And the measurement data used for parameter estimation undoubtedly include error. For example, the reanalysis of measurements made in the Netherlands by Goedhart et al. (2020) is not reflected in parameter set 2. Because the ALFAM2 model parameters are based on micrometeorological measurements only, the focus is on bLS and IHF results here.

In I-AU, the model predicted an initial flux higher than any measurements (Figure S2), but close to the value from bLS-CRDS, which were the highest among measurements. Predicted emission quickly dropped below all measurements within 6 h. Predicted cumulative emission after 8 h was below values measured with every method except DTM, which was unusually low compared to the other methods (Table 2). This comparison – particularly between the bLS methods and model – indicates that the accuracy of early predictions might be improved. Future work could evaluate partitioning of TAN within the ALFAM2 model between the lumped “slow” and “fast” pools, as well as the emission rate constant for the fast pool, r_1.

In II-WUR, predicted emission dynamics by the model were quite similar to all micrometeorological measurements, in terms of both the shape of the flux curve but also the flux magnitude (Figure S9). As with measurements, predicted flux from the model increased over the first few hours after slurry application, due to increases in both air temperature and wind speed (at least according to the model). This provides evidence that the measured increases may at least partially reflect a true response in emission rate. A scatterplot comparing flux confirms the relatively close match but shows a trend for slightly lower predictions from the model, especially when flux was high (Figure S10). As discussed above, improper injection as mentioned by Huijsmans et al. (2018) may cause overfilling slots which can lead to an increase in emission. Presently this effect is not included in model parameters. Although inclusion might improve model accuracy, slot volume is unlikely to be available as a model input, and inclusion of an improper practice is difficult to quantify in the model and only logical if it is found to be widespread.

Measured flux from bLS-CRDS measurements declined abruptly about 4 days after application (Figure S9), likely due to about 5 mm of rain that fell at that time (Fig. 7). Although the parameter set used for the model includes an effect of rainfall rate, it had a negligible effect on predicted flux in this situation and consequently the model overpredicts flux and cumulative emission. A more comprehensive evaluation of the ALFAM2 rainfall effect may be productive. Furthermore, the effect of rain is difficult to measure or model; the intensity of the rain in interaction with the soil humidity may play a role.

The under-prediction of emission by the model in I-AU suggests that actual emission may have been unusually high. Although any inference should be tempered by large apparent error in ALFAM2 predictions (11–15% of applied TAN, Hafner et al., 2021), this result highlights the importance of the performance of the application and the interaction with the soil (Hansen et al., 2003; Huijsmans et al., 2018), which is very difficult to quantify in a model. Huijsmans et al. (2018) also showed a clear soil type effect when using shallow injection, which may be also

partly due to performance on different soil types. Inclusion of slurry covered area and soil properties in data submitted to the ALFAM2 or similar databases could improve later modelling. This would of course require some simple and reliable method for quantifying slurry covered surface area. A first step could be to describe the slurry application in more detail beyond only the general categories currently included in the database and parameter set (broadcast, trailing hose, open slot injection, and closed slot injection).

5. Conclusions

Results presented here show that overall error in measurement of ammonia emission by micrometeorological methods may be 24–31 % (standard deviation) when systematic components are included. A realistic 95 % confidence interval for emission measured in a single field plot is approximately 60 % to 160 % of the measured value. Replication of a particular method will do little to reduce error if the systematic component is the largest part of overall error. Emission factors or model predictions based on multiple measurements made by multiple research groups in different locations will generally provide more precise estimates of average emission, but, unfortunately, introduce other sources of variability. Not surprisingly, differences among enclosure methods seem to be even larger than for micrometeorological, highlighting the importance of chamber operation and design on the resulting emission estimates or estimates of effect sizes. High-frequency methods like bLS-CRDS or WT-CRDS can be used to quantify emissions dynamics, facilitating research into emission processes or mechanisms of mitigation strategies. But it is not clear that high-frequency micrometeorological methods provide better accuracy in determination of total emission. The best choice of method must be evaluated according to the aim of each individual study. Future studies might aim to more clearly differentiate multiple sources of both systematic and random error using completely crossed factorial experimental designs with multiple research groups and locations, in order to better understand and ultimately reduce uncertainty associated with emission measurement.

Funding

This work was funded by the Ministry of Food, Agriculture and Fisheries of Denmark through two green development and demonstration programs (GUDP) with the project titles eGylle (journal no.: 34009-20-1751) and Methods for reducing ammonia loss and increased methane yield from biogas slurry (MAG) (journal no.: 34009-21-1829). Furthermore, this work is supported by funds from the German Government Special Purpose Fund held at Landwirtschaftliche Rentenbank (journal no.: 892976) and funded by The Ministry of Agriculture, Nature, and Food Quality (the Netherlands) with the NKS-project on ammonia losses from field-applied manures (journal no.: BO-43-101-037).

CRediT authorship contribution statement

Jesper N. Kamp: Writing – review & editing, Writing – original draft, Visualization, Validation, Methodology, Investigation, Formal analysis, Data curation, Conceptualization. **Sasha D. Hafner:** Writing – review & editing, Writing – original draft, Visualization, Validation, Methodology, Formal analysis, Data curation, Conceptualization. **Jan Huijsmans:** Writing – review & editing, Writing – original draft, Validation, Methodology, Investigation, Conceptualization. **Koen van Boheemen:** Writing – review & editing, Validation, Investigation. **Hannah Götze:** Writing – review & editing, Validation, Methodology, Investigation, Formal analysis, Conceptualization. **Andreas Pacholski:** Writing – review & editing, Validation, Methodology, Investigation, Funding acquisition, Conceptualization. **Johanna Pedersen:** Writing – review & editing, Writing – original draft, Validation, Methodology, Investigation, Formal analysis, Data curation, Conceptualization.

Declaration of competing interest

The authors declare that they have no known competing financial interests or personal relationships that could have appeared to influence the work reported in this paper.

Data availability

All emission measurement data were submitted to the ALFAM2 database and can be retrieved from v2.45 using the following plot-method keys ("pmid"): 2405, 2406, and 2407 (bLS-Impinger), 1939 & 1940 (bLS-ALPHA), 1945 (bLS-CRDS avg), 1936 & 1937 (bLS-CRDS), 1941–1943 (DTM), 1946 (IHF), 1911–1917 & 1926–1934 (WT), and 2244–2247 (FC). Calculations and data can be found in a GitHub repository (https://github.com/AU-BCE-EE/Kamp-2024-NH3FluxMethods).

Acknowledgements

Thanks to technicians Melanie Saul, Heidi Grønbæk, Leonid Mshanetskyi, and Peter Storgård Nielsen for their skillful help with carrying out the field experiments and laboratory analysis in Denmark. Thanks to Jens Bonderup Kjeldsen for drone pictures. Thanks to Heidi Grønbæk, Peter Storgård Nielsen, Ben Rutgers, Willem de Visser, Ben Verwijs, Annemieke Hol, and Paul Goedhart for their skillful help carrying out the field experiment in the Netherlands.

Supplementary materials

Supplementary material associated with this article can be found, in the online version, at doi:10.1016/j.agrformet.2024.110077.

References

Andersson, K., Delin, S., Pedersen, J., Hafner, S.D., Nyord, T., 2023. Ammonia emissions from untreated, separated and digested cattle slurry e Effects of slurry type and application strategy on a Swedish clay soil. Biosyst. Eng. 226, 194–208. https://doi.org/10.1016/j.biosystemseng.2023.01.012.

Bühler, M., Häni, C., Ammann, C., Mohn, J., Neftel, A., Schrade, S., Zähner, M., Zeyer, K., Brönnimann, S., Kupper, T., 2021. Assessment of the inverse dispersion method for the determination of methane emissions from a dairy housing. Agric. For. Meteorol. 307 https://doi.org/10.1016/j.agrformet.2021.108501.

Bates, D., Mächler, M., Bolker, B., Walker, S., 2015. Fitting linear mixed-effects models using lme4. J. Stat. Softw. 67 https://doi.org/10.18637/jss.v067.i01.

Bhandral, R., Bittman, S., Kowalenko, G., Buckley, K., Chantigny, M.H., Hunt, D.E., Bounaix, F., Friesen, A., 2009. Enhancing soil infiltration reduces gaseous emissions and improves n uptake from applied dairy slurry. J. Environ. Qual. 38, 1372–1382. https://doi.org/10.2134/jeq2008.0287.

Bobrutzki, K., von, Braban, C.F., Famulari, D., Jones, S.K., Blackall, T., Smith, T.E.L., Blom, M., Coe, H., Gallagher, M., Ghalaieny, M., McGillen, M.R., Percival, C.J., Whitehead, J.D., Ellis, R., Murphy, J., Mohacsi, A., Pogany, A., Junninen, H., Rantanen, S., Sutton, M.A., Nemitz, E., 2010. Field inter-comparison of eleven atmospheric ammonia measurement techniques. Atmos. Meas. Tech. 3, 91–112. https://doi.org/10.5194/amt-3-91-2010.

Bourdin, F., Sakrabani, R., Kibblewhite, M.G., Lanigan, G.J., 2014. Effect of slurry dry matter content, application technique and timing on emissions of ammonia and greenhouse gas from cattle slurry applied to grassland soils in Ireland. Agric. Ecosyst. Environ. 188, 122–133. https://doi.org/10.1016/j.agee.2014.02.025.

Bruggen, C. van, Bannink, A., Bleeker, A., Bussink, D.W., van Dooren, H.J.C., Groenestein, C.M., Huijsmans, J.F.M., Kros, J., Lagerwerf, L.A., Oltmer, K., Ros, M.B. H., van Schijndel, M.W., Schulte-Uebbing, L., Velthof, G.L., van der Zee, T.C., 2023. Emissies naar lucht uit de landbouw berekend met NEMA voor 1990-2021. (WOt-Technical report; no. 242) (Emissions to Air from Agriculture Calculated with NEMA for 1990-2021). doi:10.18174/629673.

Carozzi, M., Loubet, B., Acutis, M., Rana, G., Ferrara, R.M., 2013. Inverse dispersion modelling highlights the efficiency of slurry injection to reduce ammonia losses by agriculture in the Po Valley (Italy). Agric. For. Meteorol. 171–172, 306–318. https://doi.org/10.1016/j.agrformet.2012.12.012.

CBS, PBL, RIVM, W, 2023. Emissies naar lucht door de land- en tuinbouw, 1990-2021 (indicator 0099, version 35, June 2, 2023) (Emissions to air from agriculture and horticulture, 1990-2021) [WWW Document]. www.clo.nl. Centraal Bureau voor De Statistiek (CBS), Den Haag; PBL Planbureau voor De Leefomgeving, Den Haag; RIVM Rijksinstituut voor Volksgezondheid en Milieu. en Wageningen University and Research, Wageningen. URL, Bilthoven. https://www.clo.nl/indicatoren/nl0099-emissies-naar-lucht-door-de-land-en-tuinbouw?ond=20888 (accessed 6.21.23).

Chantigny, M.H., Rochette, P., Angers, D.A., Massé, D., Côté, D., 2004. Ammonia volatilization and selected soil characteristics following application of anaerobically digested pig slurry. Soil Sci. Soc. Am. J. 68, 306–312. https://doi.org/10.2136/sssaj2004.3060.

Cole, N.A, Todd, W, R, Parker, D.B, Rhoades, M.B, 2007. Challenges in Using Flux Chambers to Measure Ammonia Emissions from Simulated Feedlot Pen Surfaces and Retention Ponds. International Symposium on Air Quality and Waste Management for Agriculture, 16-19 September 2007. Broomfield, Colorado 18. https://doi.org/10.13031/2013.23827.

Evans, L., VanderZaag, A.C., Sokolov, V., Baldé, H., MacDonald, D., Wagner-Riddle, C., Gordon, R., 2018. Ammonia emissions from the field application of liquid dairy manure after anaerobic digestion or mechanical separation in Ontario. Canada. Agric For Meteorol 258, 89–95. https://doi.org/10.1016/j.agrformet.2018.02.017.

Fangueiro, D., Hjorth, M., Gioelli, F., 2015. Acidification of animal slurry– a review. J. Environ. Manage 149, 46–56. https://doi.org/10.1016/j.jenvman.2014.10.001.

Ferrara, R.M., Carozzi, M., Di Tommasi, P., Nelson, D.D., Fratini, G., Bertolini, T., Magliulo, V., Acutis, M., Rana, G., 2016. Dynamics of ammonia volatilisation measured by eddy covariance during slurry spreading in north Italy. Agric. Ecosyst. Environ. 219, 1–13. https://doi.org/10.1016/j.agee.2015.12.002.

Flesch, T.K., Wilson, J.D., Harper, L.A., Crenna, B.P., Sharpe, R.R., 2004. Deducing ground-to-air emissions from observed trace gas concentrations: J. Appl. Meteorol. 43, 487–502. https://doi.org/10.1175/1520-0450(2004)043<0487:DGEFOT>2.0.CO;2.

Flesch, T.K., Wilson, J.D., Harper, L.A., 2005a. Deducing ground-to-air emissions from observed trace gas concentrations: a field trial with wind disturbance. J. Appl. Meteorol. 44, 475–484. https://doi.org/10.1175/JAM2214.1.

Flesch, T.K., Wilson, J.D., Harper, L.A., Crenna, B.P., 2005b. Estimating gas emissions from a farm with an inverse-dispersion technique. Atmos. Environ. 39, 4863–4874. https://doi.org/10.1016/j.atmosenv.2005.04.032.

Flesch, T.K., McGinn, S.M., Chen, D., Wilson, J.D., Desjardins, R.L., 2014. Data filtering for inverse dispersion emission calculations. Agric. For. Meteorol. 198–199, 1–6. https://doi.org/10.1016/j.agrformet.2014.07.010.

Fowler, D., Coyle, M., Flechard, C., Hargreaves, K., Nemitz, E., Storeton-West, R., Sutton, M., Erisman, J.-W., 2001. Advances in micrometeorological methods for the measurement and interpretation of gas and particle nitrogen fluxes. Plant Soil. 228, 117–129.

Gao, Z., Desjardins, R.L., Flesch, T.K., 2009. Comparison of a simplified micrometeorological mass difference technique and an inverse dispersion technique for estimating methane emissions from small area sources. Agric. For. Meteorol. 149, 891–898. https://doi.org/10.1016/j.agrformet.2008.11.005.

Gao, Z., Desjardins, R.L., Flesch, T.K., 2010. Assessment of the uncertainty of using an inverse-dispersion technique to measure methane emissions from animals in a barn and in a small pen. Atmos. Environ. 44, 3128–3134. https://doi.org/10.1016/j.atmosenv.2010.05.032.

Garcia, P., Støckler, A.H., Feilberg, A., Kamp, J.N., 2024. Investigation of non-target gas interferences on a multi-gas cavity ring-down spectrometer. Atmos. Environ. X. 100258 https://doi.org/10.1016/j.aeaoa.2024.100258.

Gericke, D., Pacholski, A., Kage, H., 2011. Measurement of ammonia emissions in multi-plot field experiments. Biosyst. Eng. 108, 164–173. https://doi.org/10.1016/j.biosystemseng.2010.11.009.

Goedhart, P.W., Mosquera, J., Huijsmans, J.F.M., 2020. Estimating ammonia emission after field application of manure by the integrated horizontal flux method: a comparison of concentration and wind speed profiles. Soil. Use Manage 36, 338–350. https://doi.org/10.1111/sum.12564.

Häni, C., Sintermann, J., Kupper, T., Jocher, M., Neftel, A., 2016. Ammonia emission after slurry application to grassland in Switzerland. Atmos. Environ. 125, 92–99. https://doi.org/10.1016/j.atmosenv.2015.10.069.

Häni, C., Flechard, C., Neftel, A., Sintermann, J., Kupper, T., 2018. Accounting for field-scale dry deposition in backward Lagrangian stochastic dispersion modelling of NH3 emissions. Atmosphere (Basel) 9, 1–23. https://doi.org/10.3390/atmos9040146.

Hafner, S.D., Pacholski, A., Bittman, S., Burchill, W., Bussink, W., Chantigny, M., Carozzi, M., Génermont, S., Häni, C., Hansen, M.N., Huijsmans, J., Hunt, D., Kupper, T., Lanigan, G., Loubet, B., Misselbrook, T., Meisinger, J.J., Neftel, A., Nyord, T., Pedersen, S.V., Sintermann, J., Thompson, R.B., Vermeulen, B., Vestergaard, A.V., Voylokov, P., Williams, J.R., Sommer, S.G., 2018. The ALFAM2 database on ammonia emission from field-applied manure: description and illustrative analysis. Agric. For. Meteorol. 258, 66–79. https://doi.org/10.1016/j.agrformet.2017.11.027.

Hafner, S.D., Pacholski, A., Bittman, S., Carozzi, M., Chantigny, M., Génermont, S., Häni, C., Hansen, M.N., Huijsmans, J., Kupper, T., Misselbrook, T., Neftel, A., Nyord, T., Sommer, S.G., 2019. A flexible semi-empirical model for estimating ammonia volatilization from field-applied slurry. Atmos. Environ. 199, 474–484. https://doi.org/10.1016/j.atmosenv.2018.11.034.

Hafner, S., Nyord, T., Sommer, S.G., Adamsen, A.P.S., 2021. Estimation of Danish emission factors for ammonia from field-applied liquid manure for 1980 to 2019. Advisory Report from DCA - National Center For Food and Agriculture. Aarhus University, Denmark submitted: 23.09.2021 138.

Hafner, S.D., Kamp, J.N., Pedersen, J., 2024. Experimental and model-based comparison of wind tunnel and inverse dispersion model measurement of ammonia emission from field-applied animal slurry. Agric. For. Meteorol. 344, 109790 https://doi.org/10.1016/j.agrformet.2023.109790.

Hansen, M.N., Sommer, S.G., Madsen, N.P., 2003. Reduction of Ammonia Emission by Shallow Slurry Injection. J. Environ. Qual. 32, 1099–1104. https://doi.org/10.2134/jeq2003.1099.

Harper, L.A., Flesch, T.K., Weaver, K.H., Wilson, J.D., 2010. The Effect of Biofuel Production on Swine Farm Methane and Ammonia Emissions. J. Environ. Qual. 39, 1984–1992. https://doi.org/10.2134/jeq2010.0172.

Hensen, A., Nemitz, E., Flynn, M.J., Blatter, A., Jones, S.K., Sørensen, L.L., Hensen, B., Pryor, S.C., Jensen, B., Otjes, R.P., Cobussen, J., Loubet, B., Erisman, J.W., Gallagher, M.W., Neftel, A., Sutton, M.A., 2009. Inter-comparison of ammonia fluxes obtained using the Relaxed. Biogeosciences. 6, 2575–2588. https://doi.org/10.5194/bg-6-2575-2009.

Huijsmans, J.F.M., Hol, J.M.G., Hendriks, M.M.W.B., 2001. Effect of application technique, manure characteristics, weather and field conditions on ammonia volatilization from manure applied to grassland. Netherlands J. Agric. Sci. 49, 323–342. https://doi.org/10.1016/S1573-5214(01)80021-X.

Huijsmans, J.F.M., Hol, J.M.G., Vermeulen, G.D., 2003. Effect of application method, manure characteristics, weather and field conditions on ammonia volatilization from manure applied to arable land. Atmos. Environ. 37, 3669–3680. https://doi.org/10.1016/S1352-2310(03)00450-3.

Huijsmans, J.F.M., Vermeulen, G.D., Hol, J.M.G., Goedhart, P.W., 2018. A model for estimating seasonal trends of ammonia emission from cattle manure applied to grassland in the Netherlands. Atmos. Environ. 173, 231–238. https://doi.org/10.1016/j.atmosenv.2017.10.050.

Kai, P., Pedersen, P., Jensen, J.E., Hansen, M.N., Sommer, S.G., 2008. A whole-farm assessment of the efficacy of slurry acidification in reducing ammonia emissions. Eur. J. Agron. 28, 148–154. https://doi.org/10.1016/j.eja.2007.06.004.

Kamp, J.N., Chowdhury, A., Adamsen, A.P.S., Feilberg, A., 2019. Negligible influence of livestock contaminants and sampling system on ammonia measurements with cavity ring-down spectroscopy. Atmos. Meas. Tech. 12, 2837–2850. https://doi.org/10.5194/amt-12-2837-2019.

Kamp, J.N., Häni, C., Nyord, T., Feilberg, A., Sørensen, L.L., 2020. The aerodynamic gradient method: implications of non-simultaneous measurements at alternating heights. Atmosphere (Basel) 11, 1067. https://doi.org/10.3390/atmos11101067.

Kamp, J.N., Häni, C., Nyord, T., Feilberg, A., Sørensen, L.L., 2021. Calculation of NH3 emissions, evaluation of backward lagrangian stochastic dispersion model and aerodynamic gradient method. Atmosphere (Basel) 12, 102. https://doi.org/10.3390/atmos12010102.

Laubach, J., Taghizadeh-Toosi, A., Sherlock, R.R., Kelliher, F.M., 2012. Measuring and modelling ammonia emissions from a regular pattern of cattle urine patches. Agric. For. Meteorol. 156, 1–17. https://doi.org/10.1016/j.agrformet.2011.12.007.

Lemes, Y.M., Garcia, P., Nyord, T., Feilberg, A., Kamp, J.N., 2022. Full-scale investigation of methane and ammonia mitigation by early single-dose slurry storage acidification. ACS Agric. Sci. Technol. 2, 1196–1205. https://doi.org/10.1021/acsagscitech.2c00172.

Lemes, Yolanda Maria, Häni, C., Kamp, J.N., Feilberg, A., 2023a. Evaluation of open- and closed-path sampling systems for the determination of emission rates of NH3 and CH4 with inverse dispersion modeling. Atmos. Meas. Tech. 16, 1295–1309. https://doi.org/10.5194/amt-16-1295-2023.

Lemes, Y.M., Nyord, T., Feilberg, A., Kamp, J.N., 2023b. Effect of covering deep litter stockpiles on methane and ammonia emissions analyzed by an inverse dispersion method. Agric. Sci. Technol. 3, 399–412. https://doi.org/10.1021/acsagscitech.2c00289.

Loubet, B., Cellier, P., Flura, D., Génermont, S., 1999a. An evaluation of the wind-tunnel technique for estimating ammonia volatilization from land: part 1. analysis and improvement of accuracy. J. Agric. Eng. Res. 72, 71–81. https://doi.org/10.1006/jaer.1998.0348.

Loubet, B., Cellier, P., Génermont, S., Flura, D., 1999b. An Evaluation of the wind-tunnel technique for estimating ammonia volatilization from land: part 2. influence of the tunnel on transfer processes. J. Agric. Eng. Res. 72, 83–92. https://doi.org/10.1006/jaer.1998.0349.

Loubet, B., Génermont, S., Ferrara, R., Bedos, C., Decuq, C., Personne, E., Fanucci, O., Durand, B., Rana, G., Cellier, P., 2010. An inverse model to estimate ammonia emissions from fields. Eur. J. Soil. Sci. 61, 793–805. https://doi.org/10.1111/j.1365-2389.2010.01268.x.

Martin, N.A., Ferracci, V., Cassidy, N., Hook, J., Battersby, R.M., di Meane, E.A., Tang, Y. S., Stephens, A.C.M., Leeson, S.R., Jones, M.R., Braban, C.F., Gates, L., Hangartner, M., Stoll, J.M., Sacco, P., Pagani, D., Hoffnagle, J.A., Seitler, E., 2019. Validation of ammonia diffusive and pumped samplers in a controlled atmosphere test facility using traceable Primary Standard Gas Mixtures. Atmos. Environ. 199, 453–462. https://doi.org/10.1016/j.atmosenv.2018.11.038.

McBain, M.C., Desjardins, R.L., 2005. The evaluation of a backward Lagrangian stochastic (bLS) model to estimate greenhouse gas emissions from agricultural sources using a synthetic tracer source. Agric. For. Meteorol. 135, 61–72. https://doi.org/10.1016/j.agrformet.2005.10.003.

Milford, C., Theobald, M.R., Nemitz, E., Hargreaves, K.J., Horvath, L., Raso, J., Dämmgen, U., Neftel, A., Jones, S.K., Hensen, A., Loubet, B., Cellier, P., Sutton, M.A., 2009. Ammonia fluxes in relation to cutting and fertilization of an intensively managed grassland derived from an inter-comparison of gradient measurements. Biogeosciences. 6, 819–834. https://doi.org/10.5194/bg-6-819-2009.

Miller, J., Miller, J.C., 2018. Statistics and Chemometrics for Analytical Chemistry. Pearson Education.

Misselbrook, T.H., Hansen, M.N., 2001. Field evaluation of the equilibrium concentration technique (JTI method) for measuring ammonia emission from land spread manure or fertiliser. Atmos. Environ. 35, 3761–3768. https://doi.org/10.1016/S1352-2310(01)00169-8.

Misselbrook, T.H., Nicholson, F.A., Chambers, B.J., Johnson, R.A., 2005. Measuring ammonia emissions from land applied manure: an intercomparison of commonly used samplers and techniques. Environ. Pollut. 135, 389–397. https://doi.org/10.1016/j.envpol.2004.11.012.

Ni, K., Pacholski, A., Gericke, D., Kage, H., 2012. Analysis of ammonia losses after field application of biogas slurries by an empirical model. J. Plant Nutr. Soil Sci. 175, 253–264. https://doi.org/10.1002/jpln.201000358.

Ni, K., Köster, J.R., Seidel, A., Pacholski, A., 2015. Field measurement of ammonia emissions after nitrogen fertilization-A comparison between micrometeorological and chamber methods. Eur. J. Agron. 71, 115–122. https://doi.org/10.1016/j.eja.2015.09.004.

Nielsen, O.-K., Plejdrup, M.S., Winther, M., Mikkelsen, M.H., Nielsen, M., Gyldenkærne, S., Fauser, P., Albrektsen, R., Hjelgaard, K.H., Bruun, H.G., Thomsen, M., 2022. Annual danish informative inventory report to UNECE. Emission inventories from the base year of the protocols to year 2020. Aarhus Univ., DCE – Danish Centre Environ. Energy 494, 969.

Pacholski, A., Cai, G., Nieder, R., Richter, J., Fan, X., Zhu, Z., Roelcke, M., 2006. Calibration of a simple method for determining ammonia volatilization in the field - Comparative measurements in Henan Province. China. Nutr Cycl Agroecosyst 74, 259–273. https://doi.org/10.1007/s10705-006-9003-4.

Parker, D., Ham, J., Woodbury, B., Cai, L., Spiehs, M., Rhoades, M., Trabue, S., Casey, K., Todd, R., Cole, A., 2013. Standardization of flux chamber and wind tunnel flux measurements for quantifying volatile organic compound and ammonia emissions from area sources at animal feeding operations. Atmos. Environ. 66, 72–83. https://doi.org/10.1016/j.atmosenv.2012.03.068.

Pedersen, J., Hafner, S.D., 2023. Ammonia emissions after field application of anaerobically digested animal slurry: literature review and perspectives. Agric. Ecosyst. Environ. 357, 108697 https://doi.org/10.1016/j.agee.2023.108697.

Pedersen, J.M., Feilberg, A., Kamp, J.N., Hafner, S., Nyord, T., 2020. Ammonia emission measurement with an online wind tunnel system for evaluation of manure application techniques. Atmos. Environ. 230, 117562 https://doi.org/10.1016/j.atmosenv.2020.117562.

Pedersen, J., Nyord, T., Feilberg, A., Labouriau, R., 2021. Analysis of the effect of air temperature on ammonia emission from band application of slurry. Environ. Pollut. 282, 117055 https://doi.org/10.1016/j.envpol.2021.117055.

Pedersen, J., Hafner, S.D., Pacholski, A., Karlsson, V.I., Rong, L., Labouriau, R., Kamp, J. N., 2024. Optimized design of flux chambers for measurement of ammonia emission after field application of slurry with full-scale farm machinery. Atmos. Meas. Tech. https://doi.org/10.5194/amt-2023-212.

Pinheiro, J.C., Bates, D.M., 2000. Mixed-Effects Models in S and S-PLUS. Springer-Verlag, New York. https://doi.org/10.1007/b98882.

Possolo, A., Iyer, H.K., 2017. Invited Article: concepts and tools for the evaluation of measurement uncertainty. Rev. Sci. Instr. 88, 011301 https://doi.org/10.1063/1.4974274.

Quakernack, R., Pacholski, A., Techow, A., Herrmann, A., Taube, F., Kage, H., 2012. Ammonia volatilization and yield response of energy crops after fertilization with biogas residues in a coastal marsh of Northern Germany. Agric. Ecosyst. Environ. 160, 66–74. https://doi.org/10.1016/j.agee.2011.05.030.

R Core Team, 2023. R: a Language and Environment for Statistical Computing.

Rochette, P., Guilmette, D., Chantigny, M.H., Angers, D.A., MacDonald, J.D., Bertrand, N., Parent, L.-É., Côté, D., Gasser, M.O., 2008. Ammonia volatilization following application of pig slurry increases with slurry interception by grass foliage. Can. J. Soil Sci. 88, 585–593. https://doi.org/10.4141/CJSS07083.

Roelcke, M., Li, S.X., Tian, X.H., Gao, Y.J., Richter, J., 2002. In situ comparisons of ammonia volatilization from N fertilizers in Chinese loess soils. Nutr. Cycl. Agroecosyst. 62, 73–88. https://doi.org/10.1023/A:1015186605419.

Ruijter, F.J.de, Huijsmans, J.F.M., Rutgers, B., 2010. Ammonia volatilization from crop residues and frozen green manure crops. Atmos. Environ. 44, 3362–3368. https://doi.org/10.1016/j.atmosenv.2010.06.019.

Ryden, J.C., Lockyer, D.R., 1985. Evaluation of a system of wind tunnels for field studies of ammonia loss from grassland through volatilisation. J. Sci. Food Agric. 36, 781–788. https://doi.org/10.1002/jsfa.2740360904.

Ryden, J.C., McNeill, J.E., 1984. Application of the micrometeorological mass balance method to the determination of ammonia loss from a grazed sward. J. Sci. Food Agric. 35, 1297–1310. https://doi.org/10.1002/jsfa.2740351206.

Saha, C.K., Zhang, G., Kai, P., Bjerg, B., 2010. Effects of a partial pit ventilation system on indoor air quality and ammonia emission from a fattening pig room. Biosyst. Eng. 105, 279–287. https://doi.org/10.1016/j.biosystemseng.2009.11.006.

Scotto di Perta, E., Fiorentino, N., Gioia, L., Cervelli, E., Faugno, S., Pindozzi, S., 2019. Prolonged sampling time increases correlation between wind tunnel and integrated horizontal flux method. Agric. For. Meteorol. 265, 48–55. https://doi.org/10.1016/j.agrformet.2018.11.005.

Sheppard, L.J., Leith, I.D., Mizunuma, T., Neil Cape, J., Crossley, A., Leeson, S., Sutton, M.A., van Dijk, N., Fowler, D., 2011. Dry deposition of ammonia gas drives species change faster than wet deposition of ammonium ions: evidence from a long-term field manipulation. Glob. Chang. Biol. 17, 3589–3607. https://doi.org/10.1111/j.1365-2486.2011.02478.x.

Sintermann, J., Ammann, C., Kuhn, U., Spirig, C., Hirschberger, R., Gärtner, A., Neftel, A., 2011a. Determination of field scale ammonia emissions for common slurry spreading practice with two independent methods. Atmos. Meas. Tech. 4, 1821–1840. https://doi.org/10.5194/amt-4-1821-2011.

Sintermann, J., Spirig, C., Jordan, A., Kuhn, U., Ammann, C., Neftel, A., 2011b. Eddy covariance flux measurements of ammonia by high temperature chemical ionisation mass spectrometry. Atmos. Meas. Tech. 4, 599–616. https://doi.org/10.5194/amt-4-599-2011.

Sintermann, J., Neftel, A., Ammann, C., Häni, C., Hensen, A., Loubet, B., Flechard, C.R., 2012. Are ammonia emissions from field-applied slurry substantially over-estimated in European emission inventories? Biogeosciences 9, 1611–1632. https://doi.org/10.5194/bg-9-1611-2012.

Sintermann, J., Dietrich, K., Häni, C., Bell, M., Jocher, M., Neftel, A., 2016. A miniDOAS instrument optimised for ammonia field measurements. Atmos. Meas. Tech. 9, 2721–2734. https://doi.org/10.5194/amt-9-2721-2016.

Sommer, S.G., Misselbrook, T.H., 2016. A review of ammonia emission measured using wind tunnels compared with micrometeorological techniques. Soil Manag 32, 101–108. https://doi.org/10.1111/sum.12209.

Sommer, S.G., Génermont, S., Cellier, P., Hutchings, N.J., Olesen, J.E., Morvan, T., 2003. Processes controlling ammonia emission from livestock slurry in the field. Eur. J. Agron. 19, 465–486. https://doi.org/10.1016/S1161-0301(03)00037-6.

Tang, Y.S., Cape, J.N., Sutton, M.A., 2001. Development and types of passive samplers for monitoring atmospheric NO2 and NH3 concentrations. ScientificWorldJournal. 1, 513–529. https://doi.org/10.1100/tsw.2001.82.

Taylor, J.R., 1982. An Introduction to Error Analysis: The Study of Uncertainties in Physical Measurements. University Science Books, Mill Valley CA, USA.

ten Huf, M., Olfs, H., 2023. Evaluation of the dynamic tube method for measuring ammonia emissions after liquid manure application. Agriculture 13, 1217. https://doi.org/10.3390/agriculture13061217.

Thompson, M., Ellison, S.L.R., 2011. Dark uncertainty. Accred. Q. Assur. 16, 483–487. https://doi.org/10.1007/s00769-011-0803-0.

Toman, B., Possolo, A., 2009. Laboratory effects models for interlaboratory comparisons. Accred. Q. Assur. 14, 553–563. https://doi.org/10.1007/s00769-009-0547-2.

Twigg, M.M., Berkhout, A.J.C., Cowan, N., Crunaire, S., Dammers, E., Ebert, V., Gaudion, V., Haaima, M., Häni, C., John, L., Jones, M.R., Kamps, B., Kentisbeer, J., Kupper, T., Leeson, S.R., Leuenberger, D., Lüttschwager, N.O.B., Makkonen, U., Martin, N.A., Missler, D., Mounsor, D., 2022. Intercomparison of in situ measurements of ambient NH3 : instrument performance and application under field conditions. Atmos. Meas. Tech. 15, 6755–6787. https://doi.org/10.5194/amt-15-6755-2022.

UNECE, 1999. Protocol to abate acidification, eutrophication and ground-level Ozone [WWW Document]. URL http://www.unece.org/env/lrtap/multi_h1.html (accessed 2.16.23).

Vilms Pedersen, S., Perta, di, E.S., Hafner, S.D., Pacholski, A.S., Sommer, S.G., 2018. Evaluation of a simple, small-plot meteorological technique for measurement of ammonia emission: feasibility, costs, and recommendations. Trans. ASABe 61, 103–115. https://10.13031/trans.12445.

Webb, J., Pain, B., Bittman, S., Morgan, J., 2010. The impacts of manure application methods on emissions of ammonia, nitrous oxide and on crop response-A review. Agric. Ecosyst. Environ. 137, 39–46. https://doi.org/10.1016/j.agee.2010.01.001.

Wyer, K.E., Kelleghan, D.B., Blanes-vidal, V., Schauberger, G., Curran, T.P., 2022. Ammonia emissions from agriculture and their contribution to fine particulate matter: a review of implications for human health. J. Environ. Manage 323, 116285. https://doi.org/10.1016/j.jenvman.2022.116285.

Yang, W., Zhu, A., Zhang, J., Zhang, X., Che, W., 2016. Assessing the backward Lagrangian stochastic model for determining ammonia emissions using a synthetic source. Agric. For. Meteorol. 216, 13–19. https://doi.org/10.1016/j.agrformet.2015.09.019.

Zhu, X., Burger, M., Doane, T.a, Horwath, W.R., 2013. Ammonia oxidation pathways and nitrifier denitrification are significant sources of N2O and NO under low oxygen availability. Pnas 110, 6328–6333. https://doi.org/10.1073/pnas.1219993110.